OSSERVATORIO ASTROFISICO DI CATANIA

Systematic Calibration Procedure for the Temperature Sensors of the SiPM Interface Boards

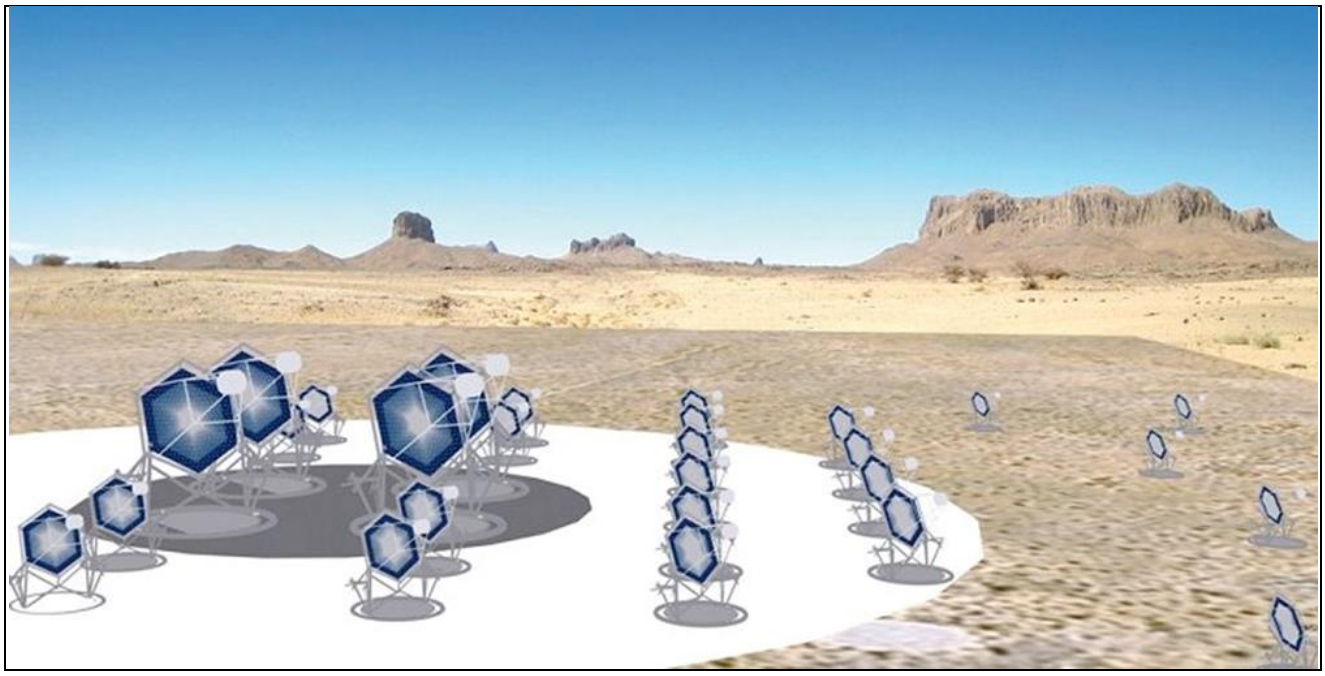

Osservatorio Astrofisico di Catania

D. MARANO[(1)], G. ROMEO[(1)], S. GAROZZO[(1)], G. BONANNO[(1)], A. GRILLO[(1)], M. C. TIMPANARO[(1)]

(1) INAF – Osservatorio Astrofisico di Catania

Rapporti interni e tecnici
N. 4/2014

INAF - Osservatorio Astrofisico di Catania
Via Santa Sofia, 78 I-95123 Catania, Italy Tel.: +39- 095-7332 111 Fax: +39-095-330592
Sede "Mario G.Fracastoro" (Etna) – Tel +39-095-911580 Fax+39-095-916184
www.oact.inaf.it - oacatania@oact.inaf.it

Systematic Calibration Procedure for the Temperature Sensors of the SiPM Interface Boards

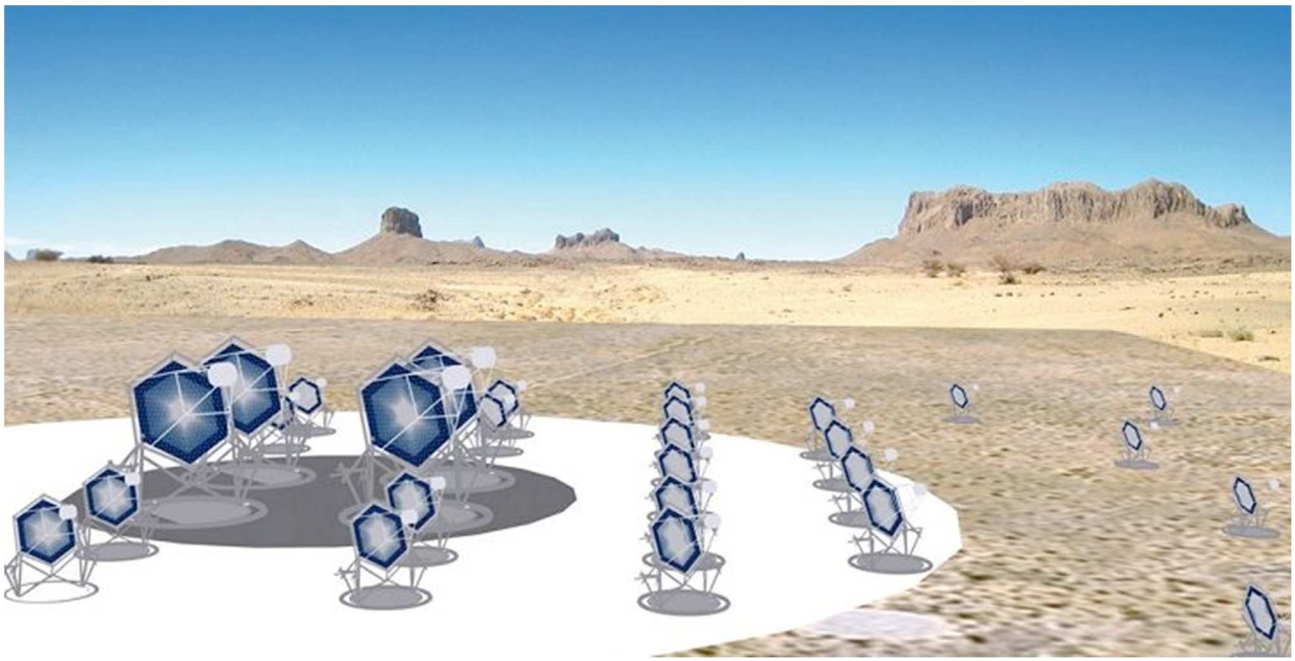

Prepared by:	Name:	Davide Marano Giuseppe Romeo Salvatore Garozzo	Signature:		Date:	25/07/2014
Reviewed by:	Name:	Giovanni Bonanno	Signature:		Date:	25/07/2014
Approved by:	Name:	Giovanni Bonanno	Signature:		Date:	25/07/2014

TABLE OF CONTENTS

DISTRIBUTION LIST **3**

DOCUMENT HISTORY **4**

LIST OF ACRONYMS **5**

APPLICABLE DOCUMENTS **5**

REFERENCE DOCUMENTS **5**

1. INTRODUCTION **6**

2. MEASUREMENT SYSTEM **7**

3. CALIBRATION CURVES **14**

4. CONCLUDING REMARKS **34**

5. CONTACTS **37**

DISTRIBUTION LIST

ASTRI mailing list	astri@brera.inaf.it
Bruno Sacco	bruno.sacco@iasf-palermo.inaf.it
Giovanni Pareschi	giovanni.pareschi@brera.inaf.it
Stefano Vercellone	stefano@ifc.inaf.it
Rodolfo Canestrari	rodolfo.canestrari@brera.inaf.it
Osvaldo Catalano	osvaldo.catalano@iasf-palermo.inaf.it
Enrico Cascone	cascone@na.astro.it
Giovanni La Rosa	larosa@ifc.inaf.it
Giovanni Bonanno	gbo@oact.inaf.it
Giuseppe Romeo	giuseppe.romeo@oact.inaf.it
Sergio Billotta	sergio.billotta@oact.inaf.it
Patrizia Caraveo	pat@lambrate.inaf.it
Davide Marano	davide.marano@oact.inaf.it
Alessandro Grillo	agrillo@oact.inaf.it
Luca Stringhetti	luca@iasf-milano.inaf.it
Rachele Millul	rachele.millul@brera.inaf.it
Mauro Fiorini	fiorini@lambrate.inaf.it
Salvatore Garozzo	salvatore.garozzo@oact.inaf.it
Domenico Impiombato	domenico.impiombato@ifc.inaf.it
Giuseppe Sottile	sottile@ifc.inaf.it
Salvatore Giarrusso	jerry@ifc.inaf.it
ASTRI mailing list	astri@brera.inaf.it

DOCUMENT HISTORY

Version	Date	Modification
1.0	Date	first version
		update

LIST OF ACRONYMS

OACT	Osservatorio Astrofisico di Catania
IFC	Istituto di Astrofisica Spaziale e Fisica Cosmica di Palermo
COLD	Catania astrophysical Observatory Laboratory for Detectors
SiPM	Silicon Photo-Multiplier
MPPC	Multi Pixel Photon Counter
SST-2M	Small-Size Telescope Dual-Mirror
PDM	Photon Detection Module
ASIC	Application Specific Integrated Circuit
FEE	Front-End Electronics
BEE	Back-End Electronics
FPGA	Field Programmable Gate Array
EASIROC	Extended Analogue Silicon-pm Integrated Read-Out Chip
CITIROC	Cherenkov Imaging Telescope Integrated Read-Out Chip
I/F	Interface

APPLICABLE DOCUMENTS

[AD1]

REFERENCE DOCUMENTS

[R1] LM-60 reference datasheet: http://www.ti.com.cn/cn/lit/ds/symlink/lm60.pdf

[R2] Distribuzione delle PDM sul piano focale della camera ASTRI e layout di ogni singola PDM – code: ASTRI-TR-OACT-3200-012.

[R3] SiPM Interface Systems for the Characterization of Complete PDMs of the ASTRI SST-2M Camera – code: ASTRI-TR-OACT-3200-014.

[R4] Reliability Tests of all 37 SiPM Boards of the ASTRI SST-2M Camera through Pulse Height Distribution Measurements – code: ASTRI-TR-OACT-3200-015.

1. INTRODUCTION

In this document the systematic procedure devoted to the complete calibration of the temperature sensors of each Photon Detection Module (PDM) at the focal plane of the ASTRI SST-2M telescope is illustrated.

The temperature sensors in each SiPM board belong to the LM-60 series by Texas Instruments [R1]. They are precision integrated-circuit sensors allowing temperature sensing from -40°C to +125°C while operating from a single +2.7-V power supply. LM-60 sensors are calibrated to provide accuracies of ±2°C at room temperature.

The temperature sensors calibration of the PDM modules constituting the focal plane of the ASTRI SST-2M telescope is essential prerequisite for the MPPC sensors gain equalization, through the input DACs of the CITIROC front-end ASICs, managed by the front-end FPGA.

Calibration of the central rear side temperature sensor of each PDM is performed, so that the remaining sensors of each board can be calibrated based on the calibrated one.

2. MEASUREMENT SYSTEM

The instrumental apparatus developed at the COLD laboratory has been envisaged to provide a systematic characterization of each SiPM board constituting the camera focal plane of the ASTRI SST-2M telescope prototype.

The calibration process of the temperature sensors on chip of the SiPM interface (I/F) boards of the ASTRI focal plane is obtained by means of two testing systems:

1. the electronic board developed at the COLD laboratory, called “adapter board”, used for SiPM macro-pixels preliminary tests;
2. a calibrated reference photodiode, manufactured by LakeShore and biased by an appropriate temperature controller developed by the company itself.

As shown in Fig. 1, the adapter board is capable of addressing manually each of the 10 temperature sensors through a dip-switch assembled on the top layer, that drives an analog multiplexer located on each SiPM I/F board, as shown in Fig. 2 [R3].

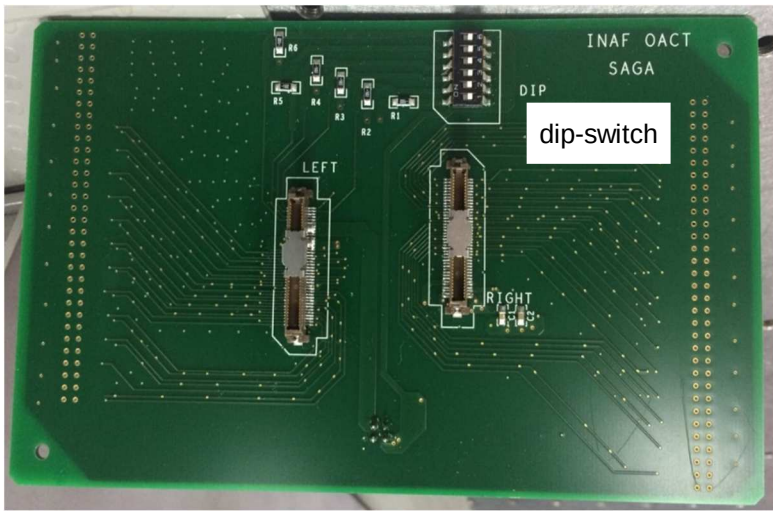

Fig. 1. Top side of the adapter board. On the upper central part the dip-switch is evident.

Each I/F board has in total 10 temperature sensors: 9 located on the rear side and 1 located at the center of the front side. We decided to calibrate only the central sensor at the bottom of the board, allowing calibration of the other 8 sensors in the bottom side of the board to be easily accomplished with respect to the calibrated one.

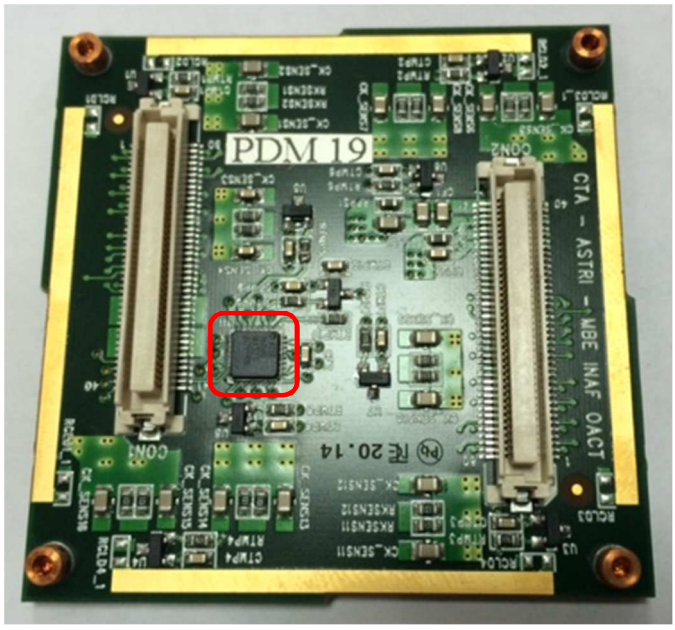

Fig. 2. Bottom side of the *n*-th SiPM I/F board. Near the upper connector, the analog multiplexer can be recognized (highlighted with a red box).

A specific mechanical support is realized to house the MPPC board; in particular, the black light-tight prevents accidental light exposure of the MPPC detectors and allows a thermal stabilization. The temperature control of the SiPM I/F is obtained through a cooling system designed at the COLD laboratory of INAF-OACT, based on a Peltier cell whose hot side is cooled by a CPU fan (see Fig. 3).

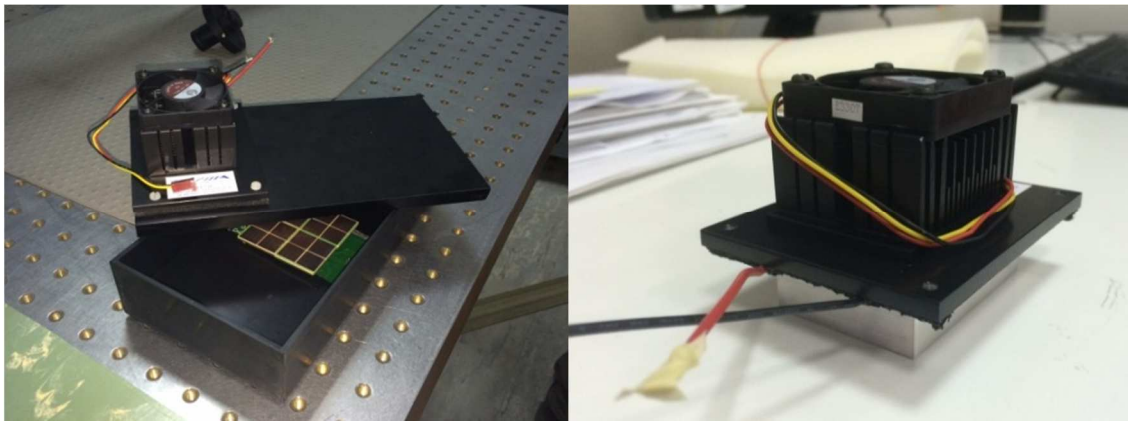

Fig. 3. The left side shows the box hosting the adapter board and the SiPM I/F board connected onto it. On the right side, the thermoelectric cooler based on a Peliter cell is depicted.

For the Peltier cell and the fan, a dual power supply is used. The system is able to maintain the temperature stable in the 25-10°C range with the possibility of setting the working temperature in steps of 0.5°C.

The temperature sensor located on the center of the bottom SiPM I/F board is calibrated by using a complete system manufactured by LakeShore, consisting of a calibrated temperature diode and an *ad-hoc* driver. Particular care is taken in placing the calibrated diode very close to each temperature sensor. In Fig. 4 the LakeShore controller and the calibrated diode are illustrated.

Fig. 4. LakeShore temperature measurement system. On the blue box, the calibrated diode.

Fig. 5 reports the plot of the typical voltage values of a DT-470 diode temperature sensor, while the standard curve delivered with the calibrated diode is reported in Fig. 6.

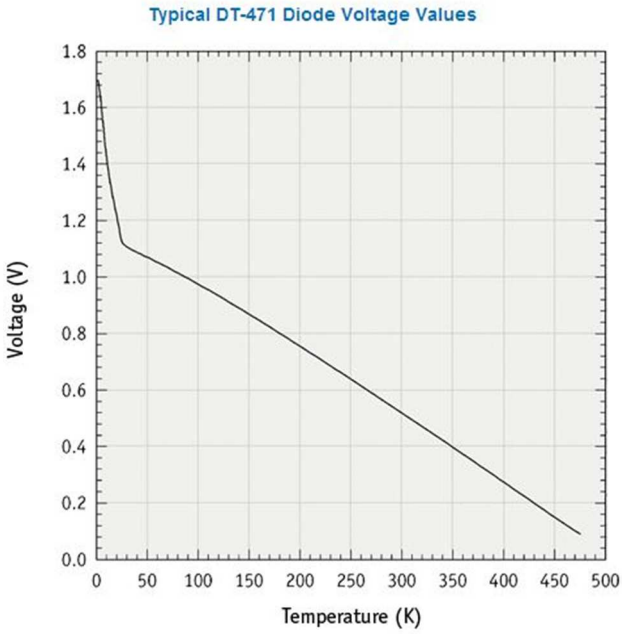

Fig. 5. Typical curve of the DT-470 calibrated temperature sensor.

T (K)	Voltage (V)	dV/dT (mV/K)	T (K)	Voltage (V)	dV/dT (mV/K)	T (K)	Voltage (V)	dV/dT (mV/K)	T (K)	Voltage (V)	dV/dT (mV/K)
1.40	1.69812	-13.1	11.5	1.38021	-24.8	38.0	1.09131	-1.77	210.0	0.73238	-2.32
1.60	1.69521	-15.9	12.0	1.36809	-23.7	40.0	1.08781	-1.74	220.0	0.70908	-2.34
1.80	1.69177	-18.4	12.5	1.35647	-22.8	42.0	1.08436	-1.72	230.0	0.68564	-2.35
2.00	1.68786	-20.7	13.0	1.34530	-21.9	44.0	1.08093	-1.72	240.0	0.66208	-2.36
2.20	1.68352	-22.7	13.5	1.33453	-21.2	46.0	1.07748	-1.73	250.0	0.63841	-2.37
2.40	1.67880	-24.4	14.0	1.32412	-20.5	48.0	1.07402	-1.74	260.0	0.61465	-2.38
2.60	1.67376	-25.9	14.5	1.31403	-19.9	50.0	1.07053	-1.75	270.0	0.59080	-2.39
2.80	1.66845	-27.1	15.0	1.30422	-19.4	52.0	1.06700	-1.77	273.15	0.58327	-2.39
3.00	1.66292	-28.1	15.5	1.29464	-18.9	54.0	1.06346	-1.78	280.0	0.56690	-2.39
3.20	1.65721	-29.0	16.0	1.28527	-18.6	56.0	1.05988	-1.79	290.0	0.54294	-2.40
3.40	1.65134	-29.8	16.5	1.27607	-18.2	58.0	1.05629	-1.80	300.0	0.51892	-2.40
3.60	1.64529	-30.7	17.0	1.26702	-18.0	60.0	1.05267	-1.81	305.0	0.50688	-2.41
3.80	1.63905	-31.6	17.5	1.25810	-17.7	65.0	1.04353	-1.84	310.0	0.49484	-2.41
4.00	1.63263	-32.7	18.0	1.24928	-17.6	70.0	1.03425	-1.87	320.0	0.47069	-2.42
4.20	1.62602	-33.6	18.5	1.24053	-17.4	75.0	1.02482	-1.91	330.0	0.44647	-2.42
4.40	1.61920	-34.6	19.0	1.23184	-17.4	77.35	1.02032	-1.92	340.0	0.42221	-2.43
4.60	1.61220	-35.4	19.5	1.22314	-17.4	80.0	1.01525	-1.93	350.0	0.39783	-2.44
4.80	1.60506	-36.0	20.0	1.21440	-17.6	85.0	1.00552	-1.96	360.0	0.37337	-2.45
5.00	1.59782	-36.5	21.0	1.19645	-18.5	90.0	0.99565	-1.99	370.0	0.34881	-2.46
5.50	1.57928	-37.6	22.0	1.17705	-20.6	95.0	0.98564	-2.02	380.0	0.32416	-2.47
6.00	1.56027	-38.4	23.0	1.15558	-21.7	100.0	0.97550	-2.04	390.0	0.29941	-2.48
6.50	1.54097	-38.7	24.0	1.13598	-15.9	110.0	0.95487	-2.08	400.0	0.27456	-2.49
7.00	1.52166	-38.4	25.0	1.12463	-7.72	120.0	0.93383	-2.12	410.0	0.24963	-2.50
7.50	1.50272	-37.3	26.0	1.11896	-4.34	130.0	0.91243	-2.16	420.0	0.22463	-2.50
8.00	1.48443	-35.8	27.0	1.11517	-3.34	140.0	0.89072	-2.19	430.0	0.19961	-2.50
8.50	1.46700	-34.0	28.0	1.11212	-2.82	150.0	0.86873	-2.21	440.0	0.17464	-2.49
9.00	1.45048	-32.1	29.0	1.10945	-2.53	160.0	0.84650	-2.24	450.0	0.14985	-2.46
9.50	1.43488	-30.3	30.0	1.10702	-2.34	170.0	0.82404	-2.26	460.0	0.12547	-2.41
10.0	1.42013	-28.7	32.0	1.10263	-2.08	180.0	0.80138	-2.28	470.0	0.10191	-2.30
10.5	1.40615	-27.2	34.0	1.09864	-1.92	190.0	0.77855	-2.29	475.0	0.09062	-2.22
11.0	1.39287	-25.9	36.0	1.09490	-1.83	200.0	0.75554	-2.31	*Partial conformances*		

Fig. 6. Standard curve of the calibrated diode DT-470.

A light shield is realized on top of the adapter board in order to prevent light penetration through the back of the black-box, and helps to maintain stable the temperature inside the box, avoiding the heat exchange with the outside of the box.

The calibrated temperature diode is positioned on top of the light-tight shield, between the two multi-pin connectors of the adapter board, as depicted in Fig. 7. This ensures that the calibrator diode and the sensors to be calibrated are very close to each other.

The I/F board is then connected to the adapter board as in Fig. 8.

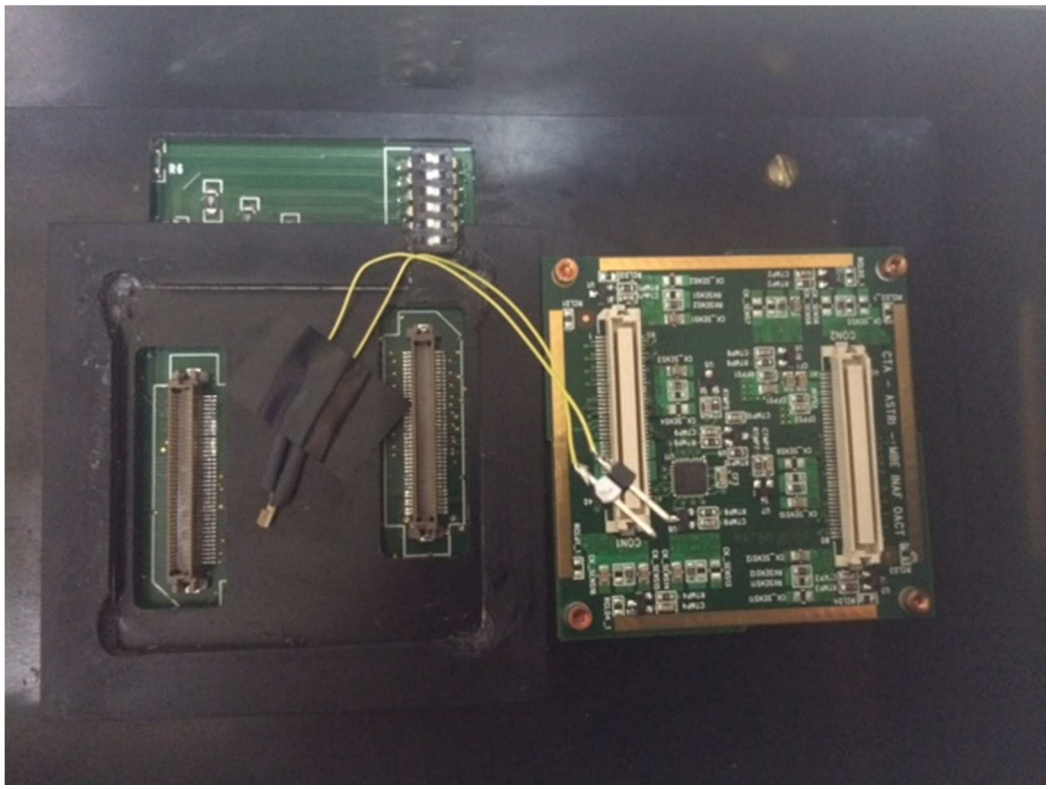

Fig. 7. Positioning of the calibrated temperature diode on top of the light-tight shield.

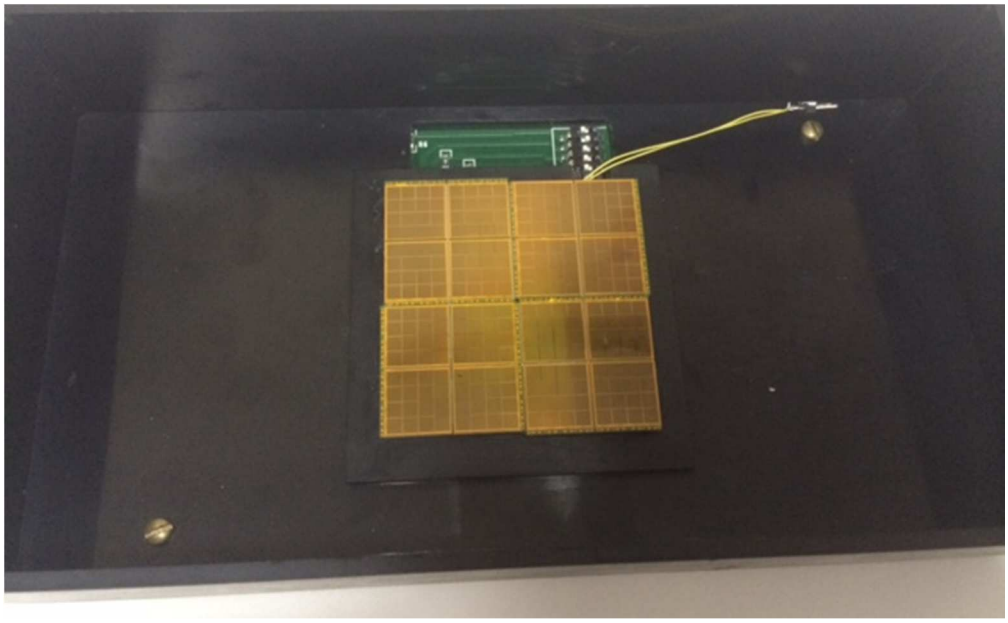

Fig. 8. SiPM I/F board connected to the adapter board inside the light-tight box.

The outputs of the calibrated diode are connected to the input of the LakeShore temperature controller. On the cool metallic plate of the Peltier cell a thin copper foil is connected to facilitate cooling inside the black box and speed up measurements, as shown in Fig. 9. Few millimeters separate the detection surface of the I/F board from the copper foil.

In order to improve the cooling process, an air-to-direct Peltier system, manufactured by Laird and shown in Fig. 10, is placed on the bottom of the black box, allowing lower values of temperature to be quickly reached.

The procedure followed for the temperature sensors calibration consists in measuring the temperature of the calibrator diode and the corresponding voltage acquired by a voltmeter of the LM-60 sensors of the I/F boards.

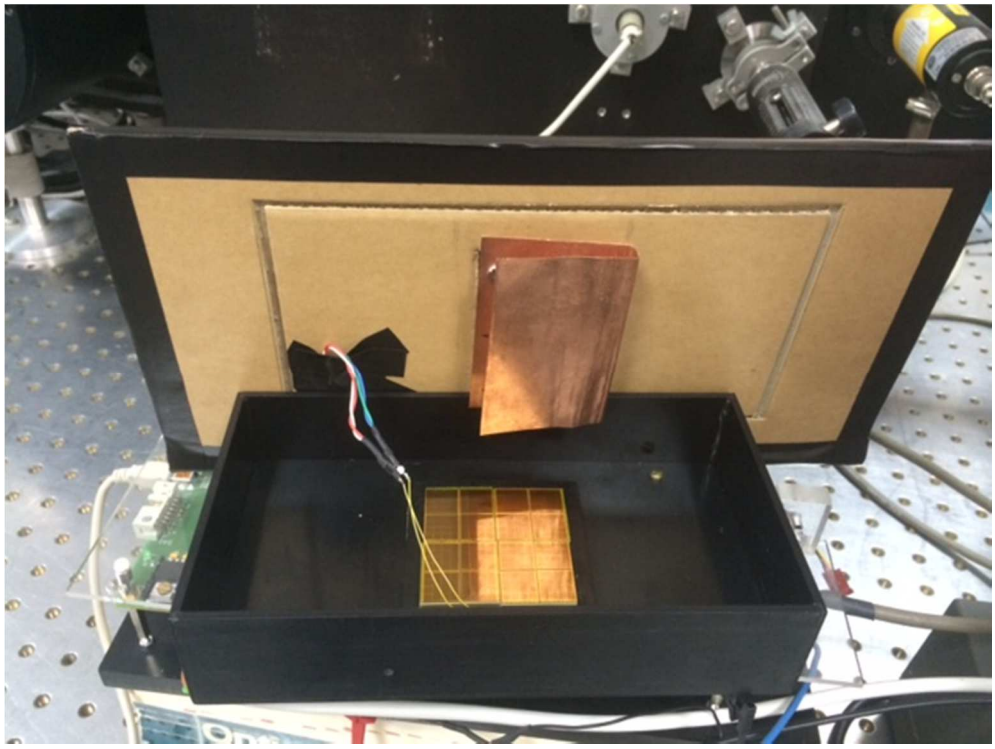

Fig. 9. Copper foil connected to the cool metallic surface of the Peltier cell.

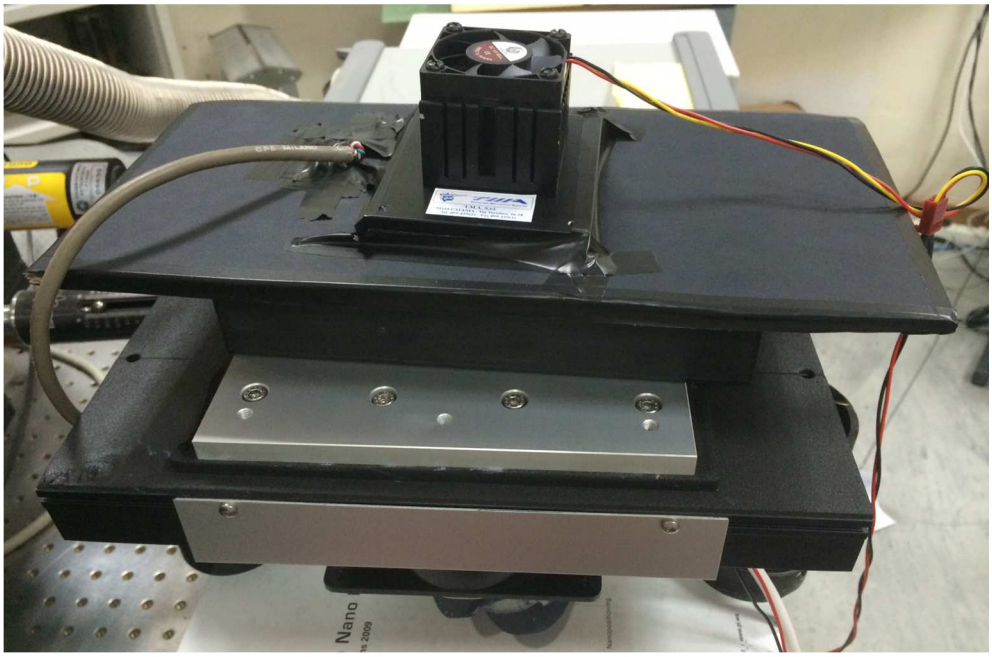

Fig. 10. Peltier cell connected to the bottom of the black box to empower the cooling process.

3. CALIBRATION CURVES

Hereby, two different sets of measurements are performed: the first one for decreasing values of the temperature *T* from 25.5°C to 10.0°C, and the second one for increasing values of *T* from 10.0°C to 25.5°C.

Acquisition is taken considering each temperature of the calibrator in steps of 0.5°C as a reference value.

For each SiPM board, the two obtained curves (one for decreasing values of *T* and one for increasing values of *T*) are plotted on Excel along with their linearized lines. For each temperature *T*, average values and fitting curves are also graphed.

However, the curves corresponding to increasing values of *T* are believed to be more accurate, because the entire calibration system spent much higher time for increasing temperature and turned out to be more controllable in temperature. A complete acquisition cycle for both falling and rising phases of temperature is estimated to be around 1 hour. (~15 minutes for increasing *T* and ~45 minutes for decreasing *T*).

In the following, the calibration results of the 37 SiPM I/F boards of the focal plane are reported. The various SiPM boards numbers are referenced through the distribution schematization depicted in Fig. 11 [R2].

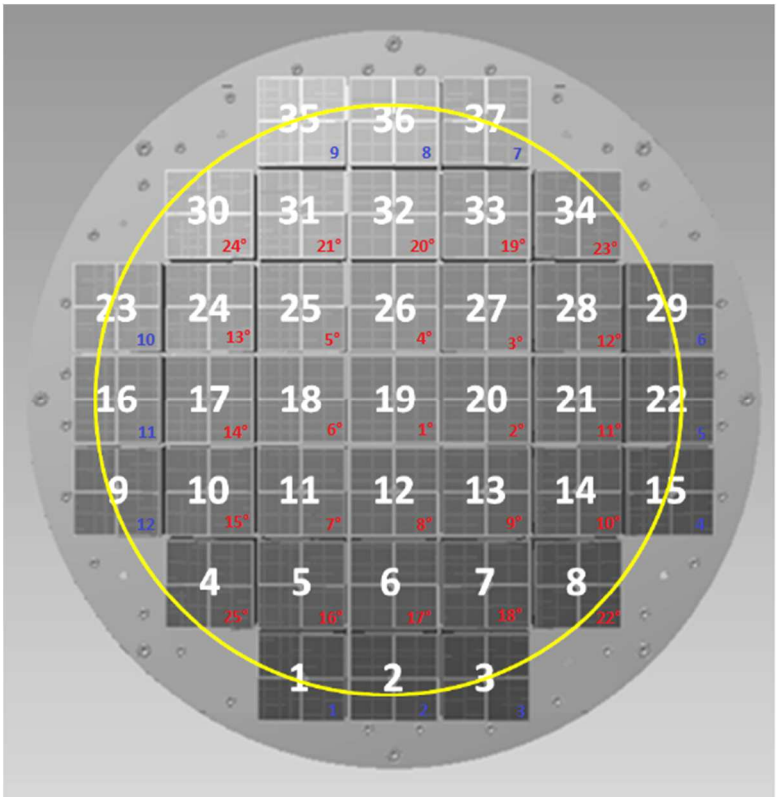

Fig. 11. PDM reference distribution at the focal plane of the ASTRI SST-2M camera.

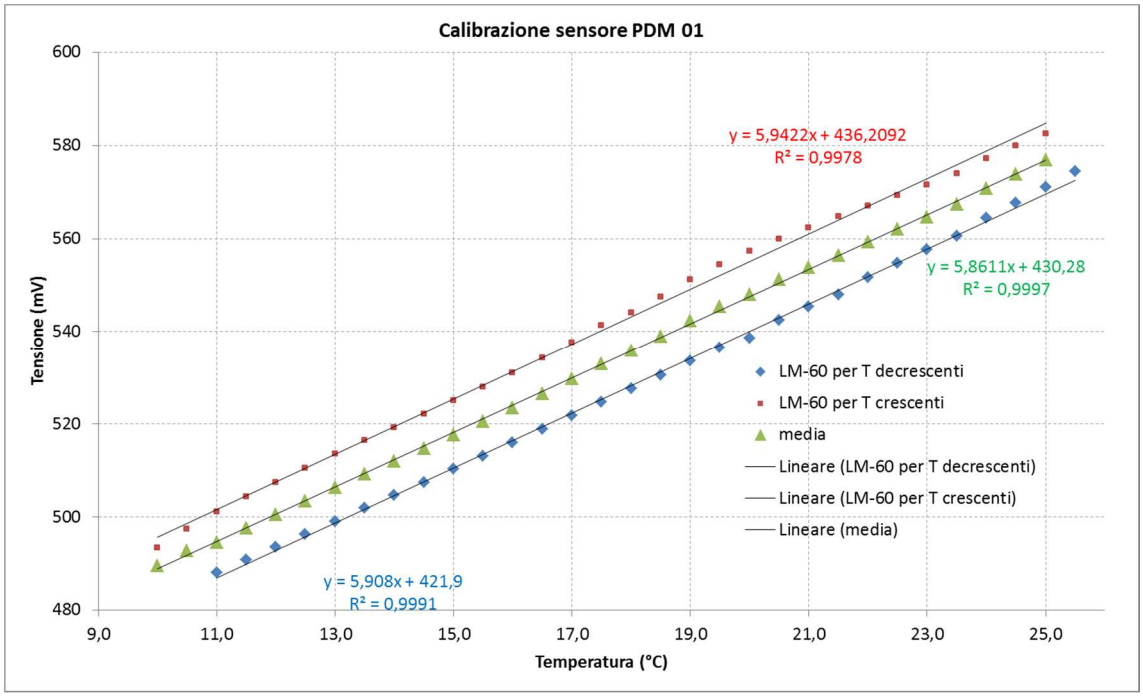

Fig. 12. Calibration curves for the LM-60 temperature sensor of the PDM 01.

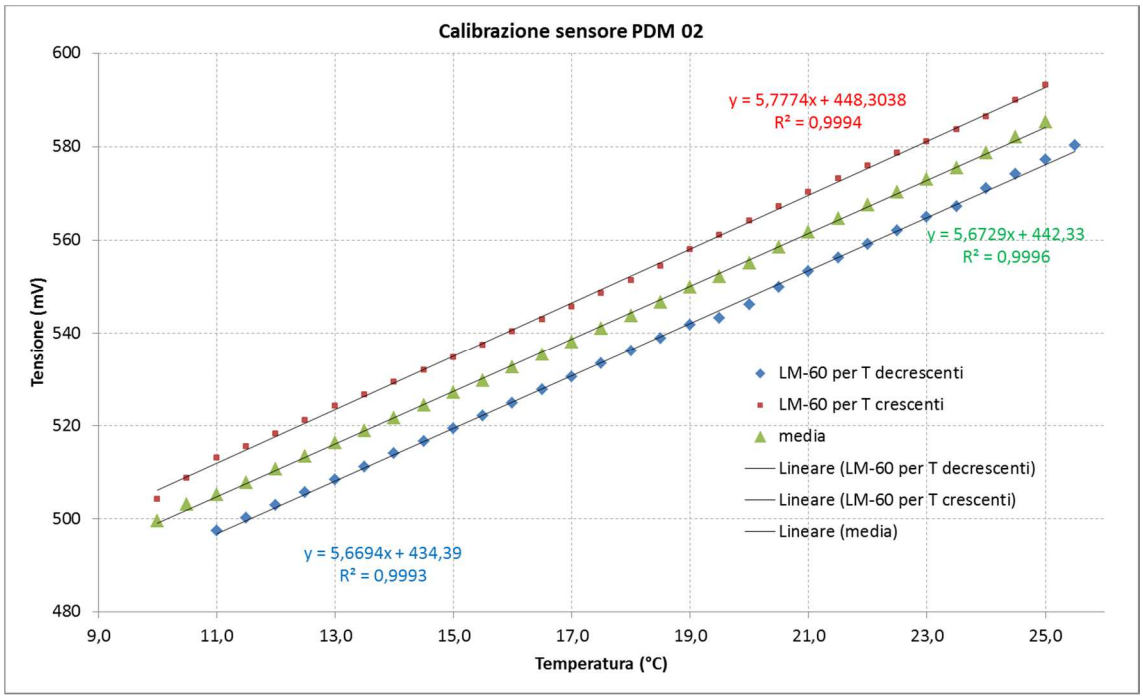

Fig. 13. Calibration curves for the LM-60 temperature sensor of the PDM 02.

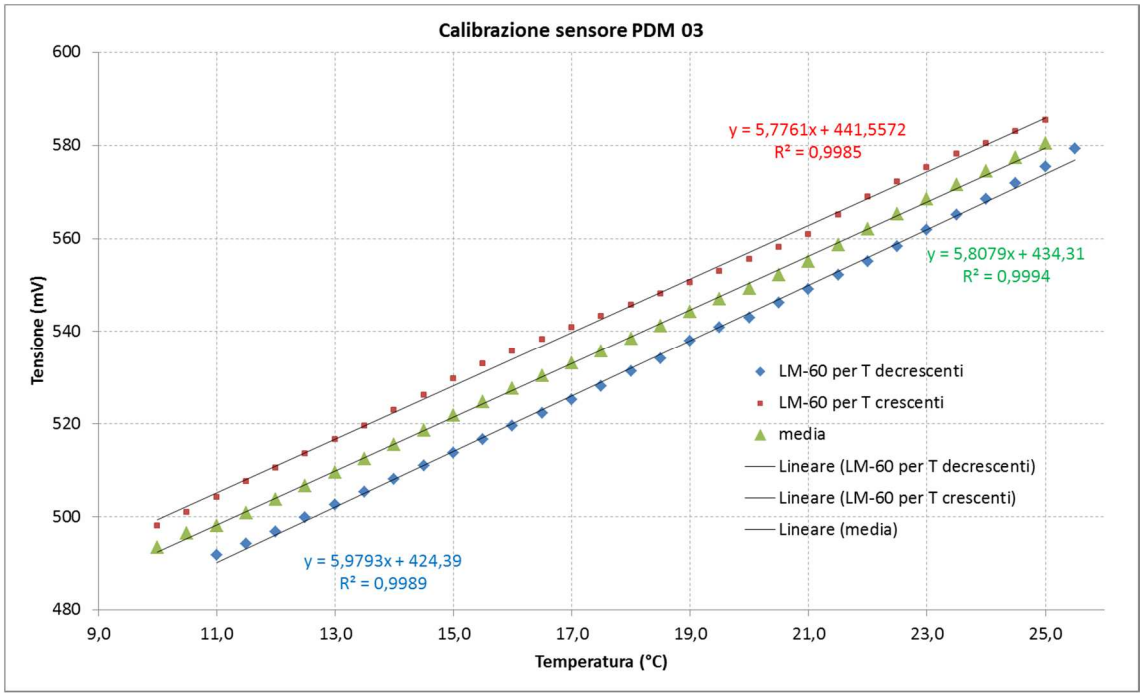

Fig. 14. Calibration curves for the LM-60 temperature sensor of the PDM 03.

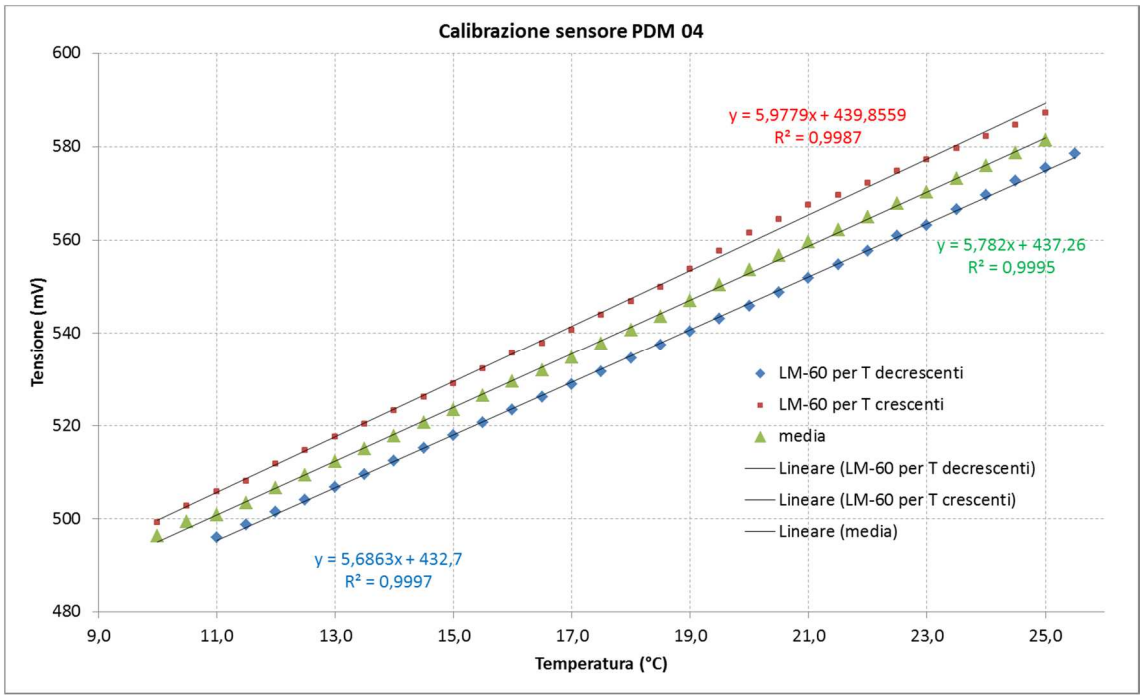

Fig. 15. Calibration curves for the LM-60 temperature sensor of the PDM 04.

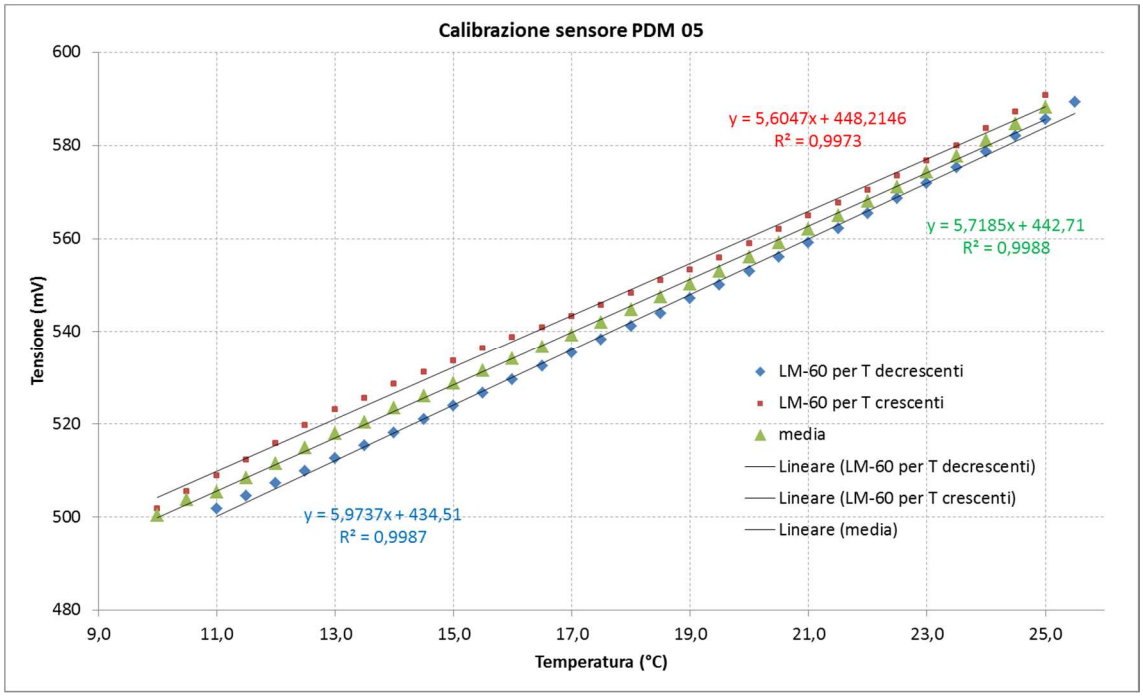

Fig. 16. Calibration curves for the LM-60 temperature sensor of the PDM 05.

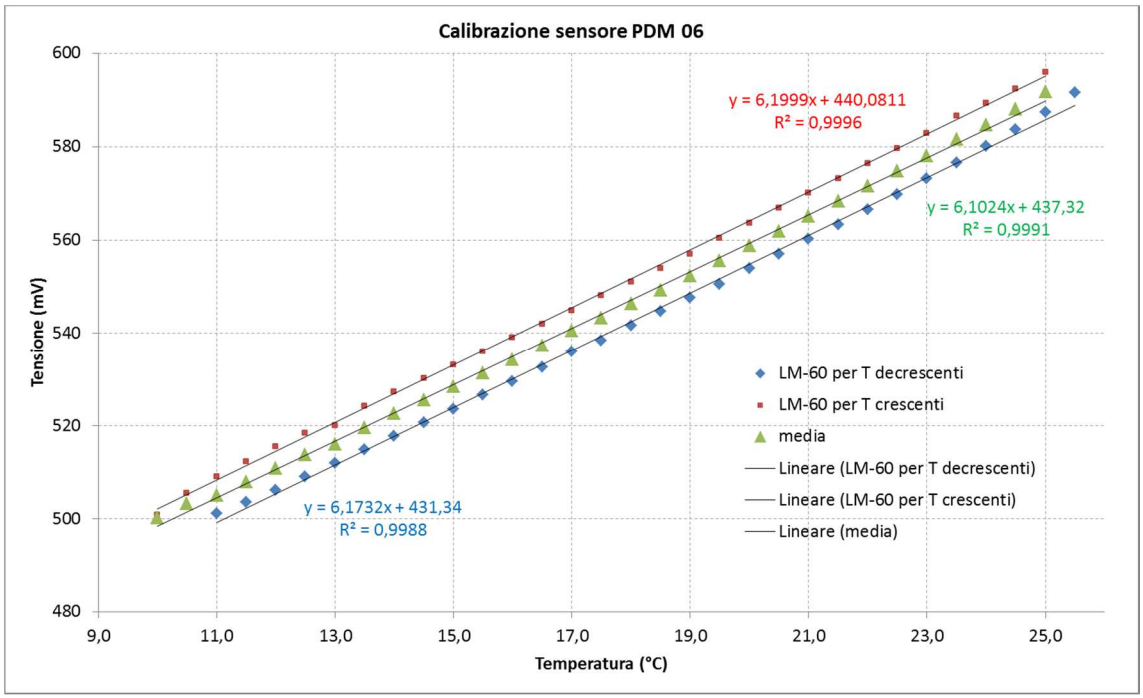

Fig. 17. Calibration curves for the LM-60 temperature sensor of the PDM 06.

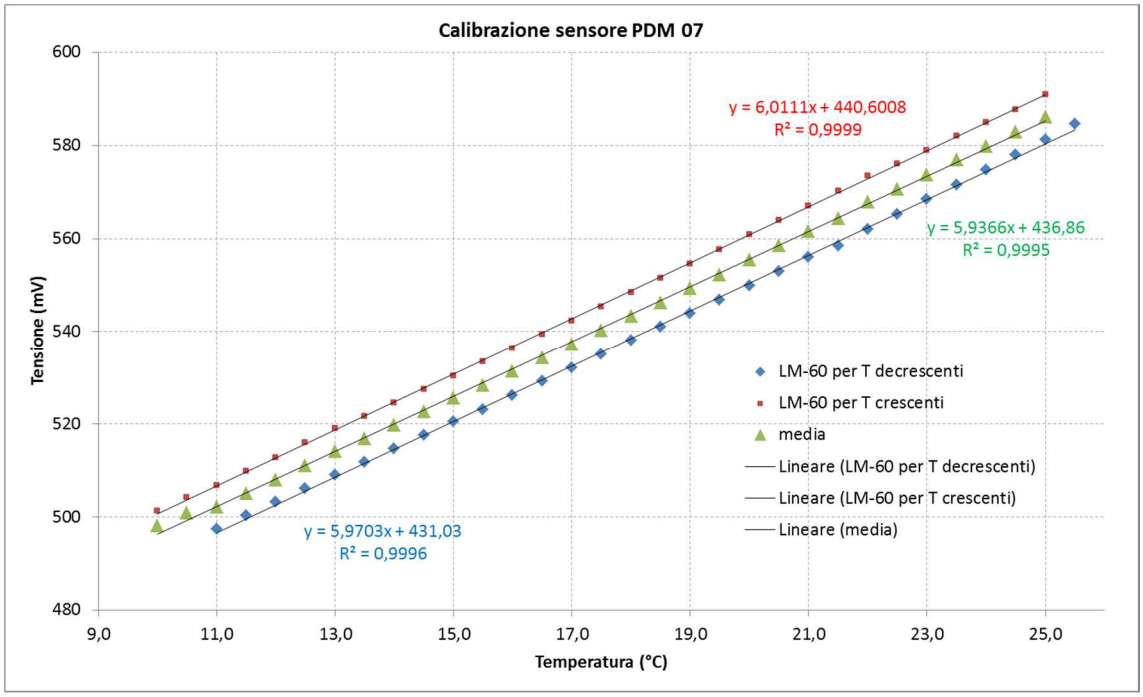

Fig. 18. Calibration curves for the LM-60 temperature sensor of the PDM 07.

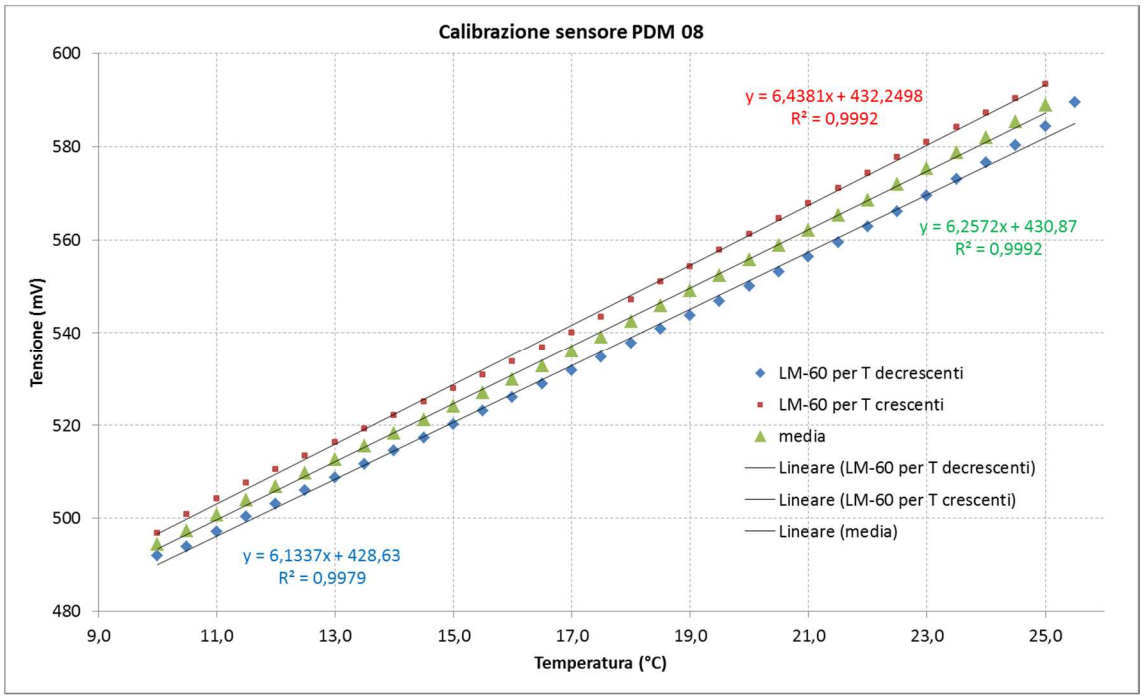

Fig. 19. Calibration curves for the LM-60 temperature sensor of the PDM 08.

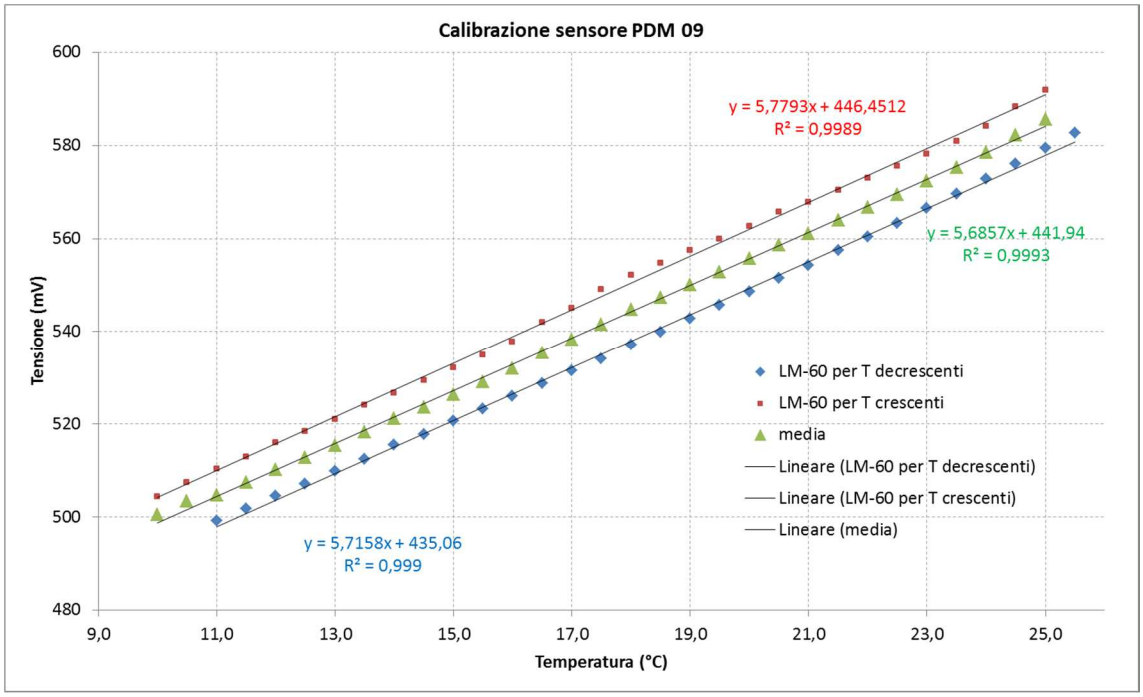

Fig. 20. Calibration curves for the LM-60 temperature sensor of the PDM 09.

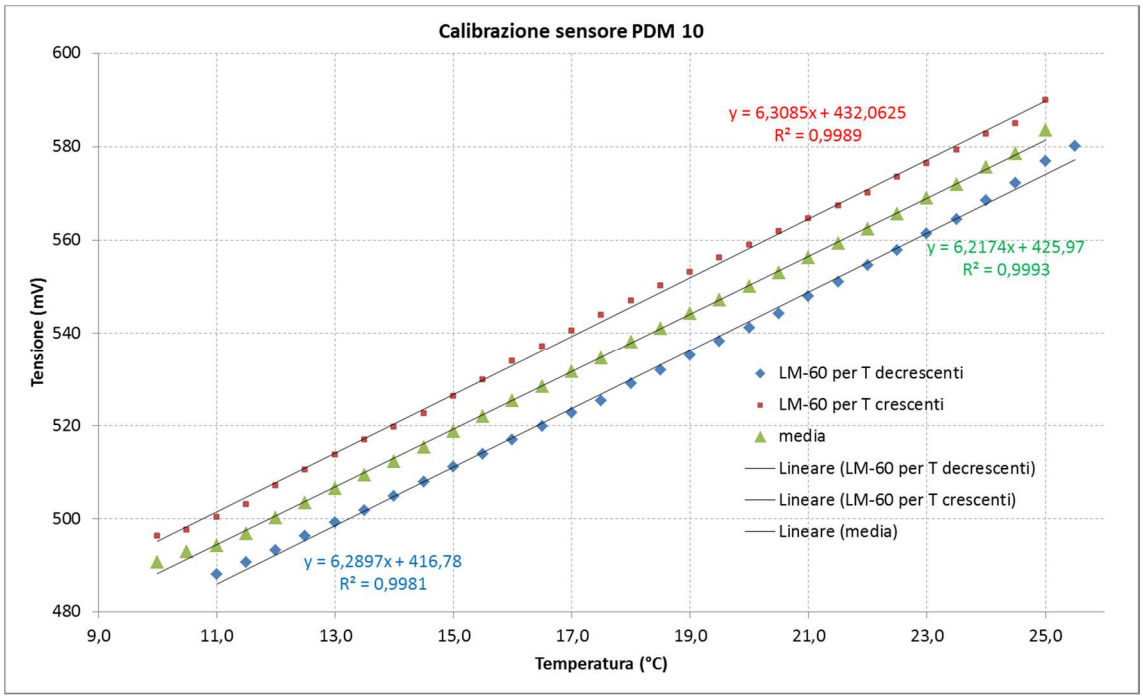

Fig. 21. Calibration curves for the LM-60 temperature sensor of the PDM 10.

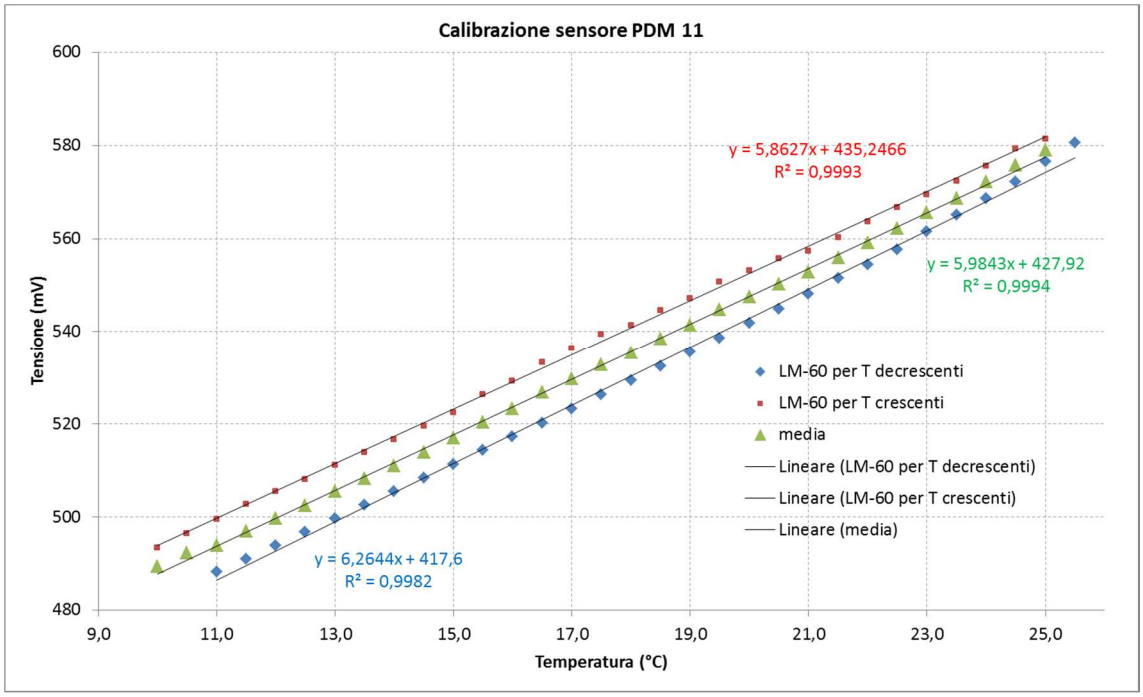

Fig. 22. Calibration curves for the LM-60 temperature sensor of the PDM 11.

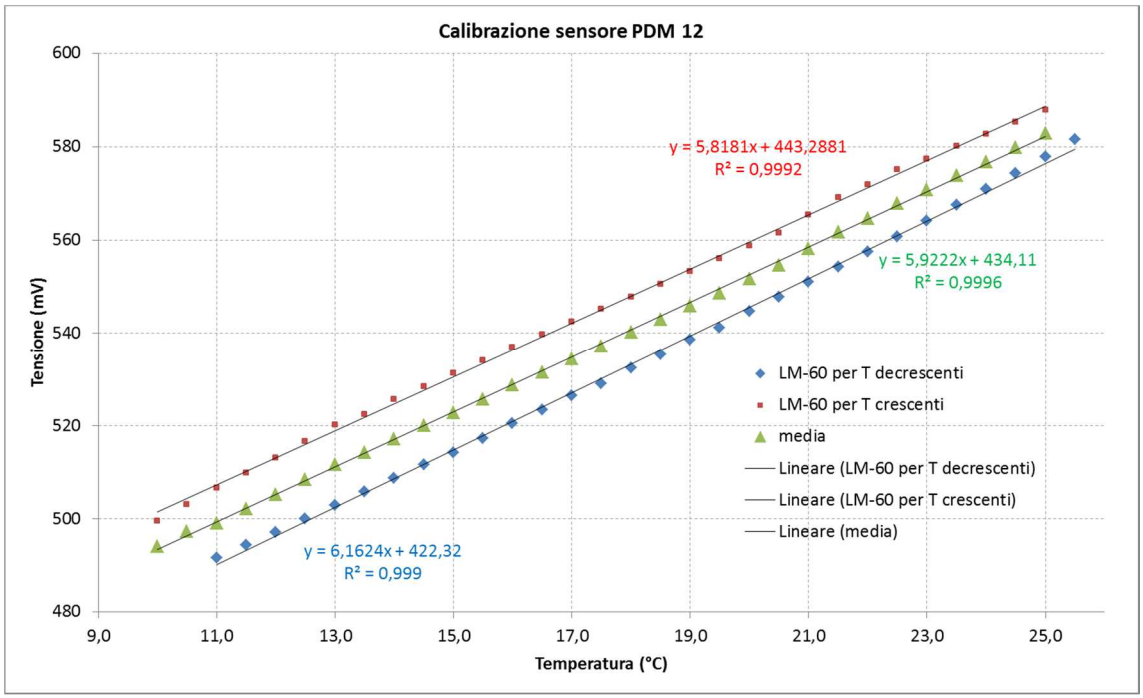

Fig. 23. Calibration curves for the LM-60 temperature sensor of the PDM 12.

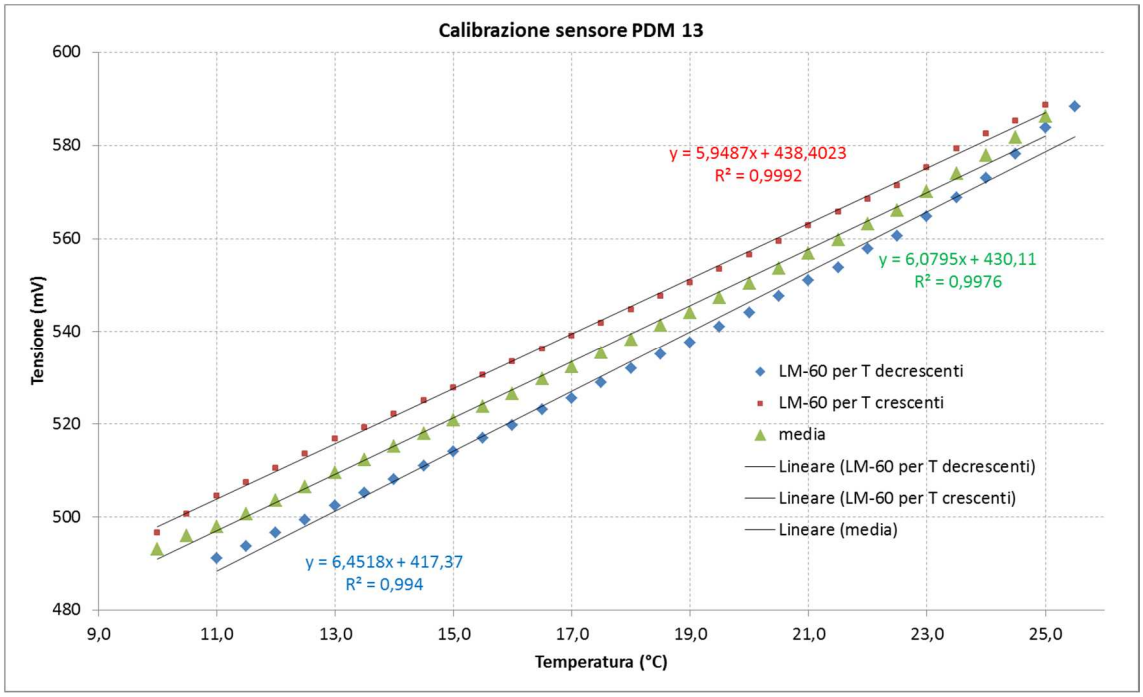

Fig. 24. Calibration curves for the LM-60 temperature sensor of the PDM 13.

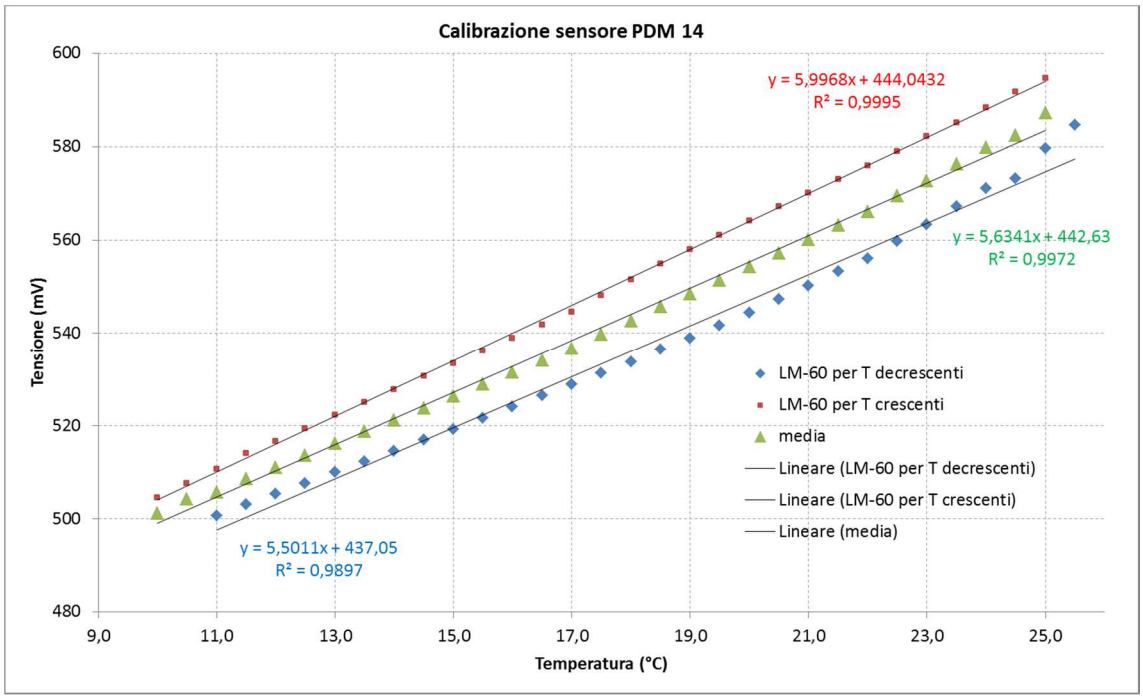

Fig. 25. Calibration curves for the LM-60 temperature sensor of the PDM 14.

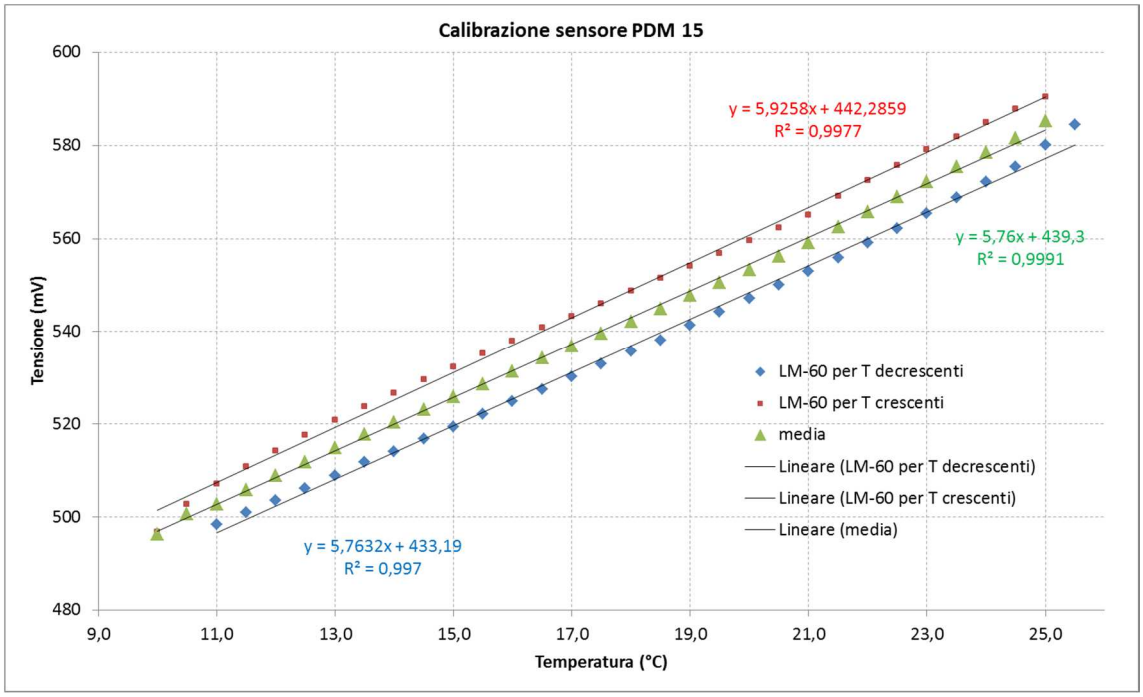

Fig. 26. Calibration curves for the LM-60 temperature sensor of the PDM 15.

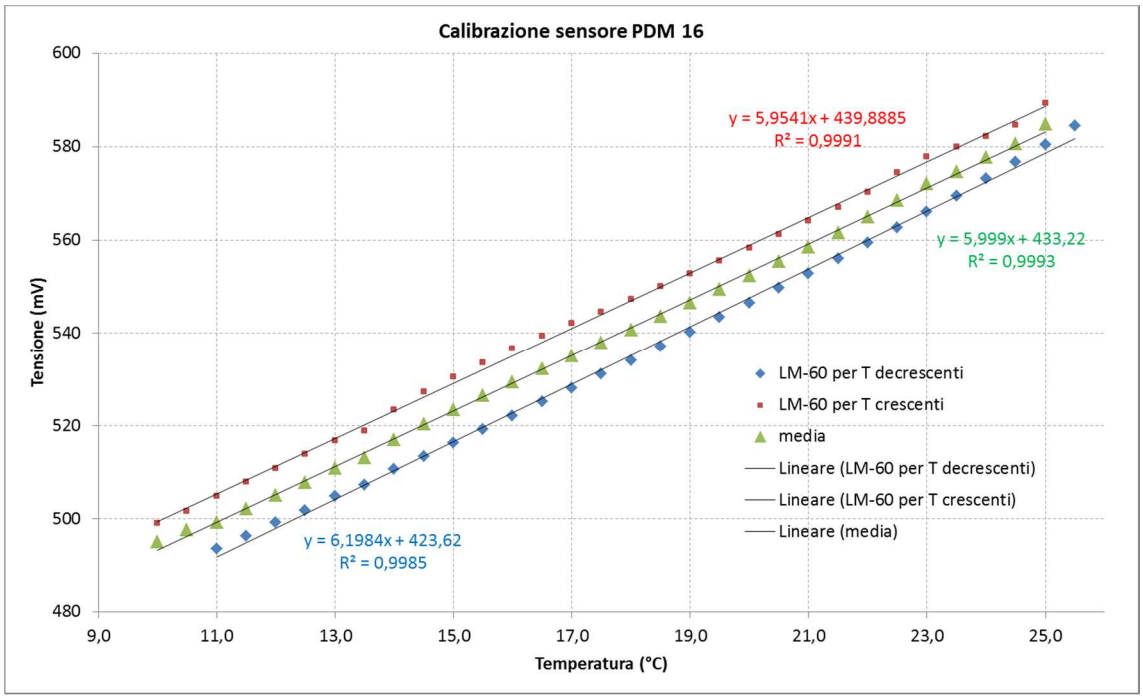

Fig. 27. Calibration curves for the LM-60 temperature sensor of the PDM 16.

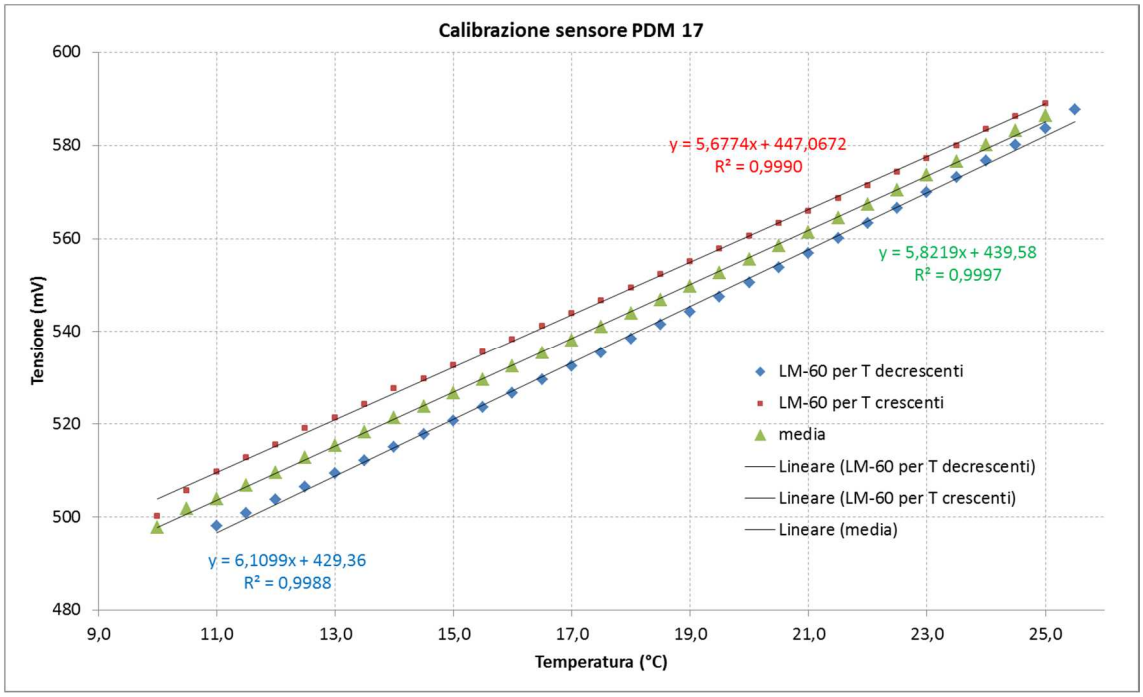

Fig. 28. Calibration curves for the LM-60 temperature sensor of the PDM 17.

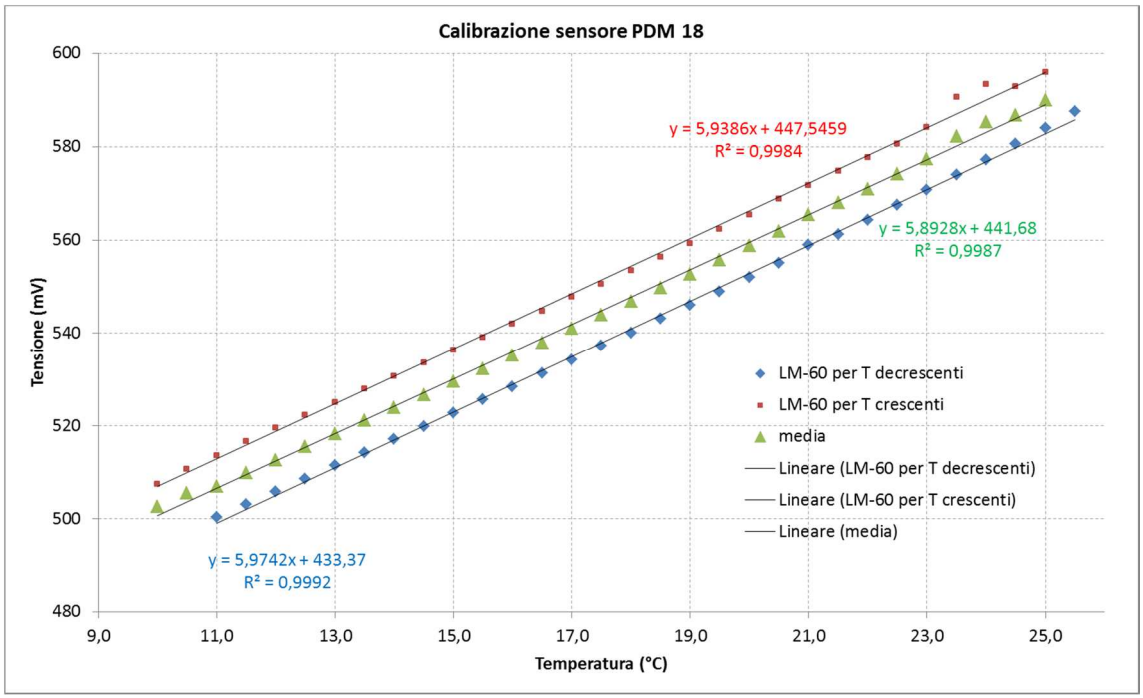

Fig. 29. Calibration curves for the LM-60 temperature sensor of the PDM 18.

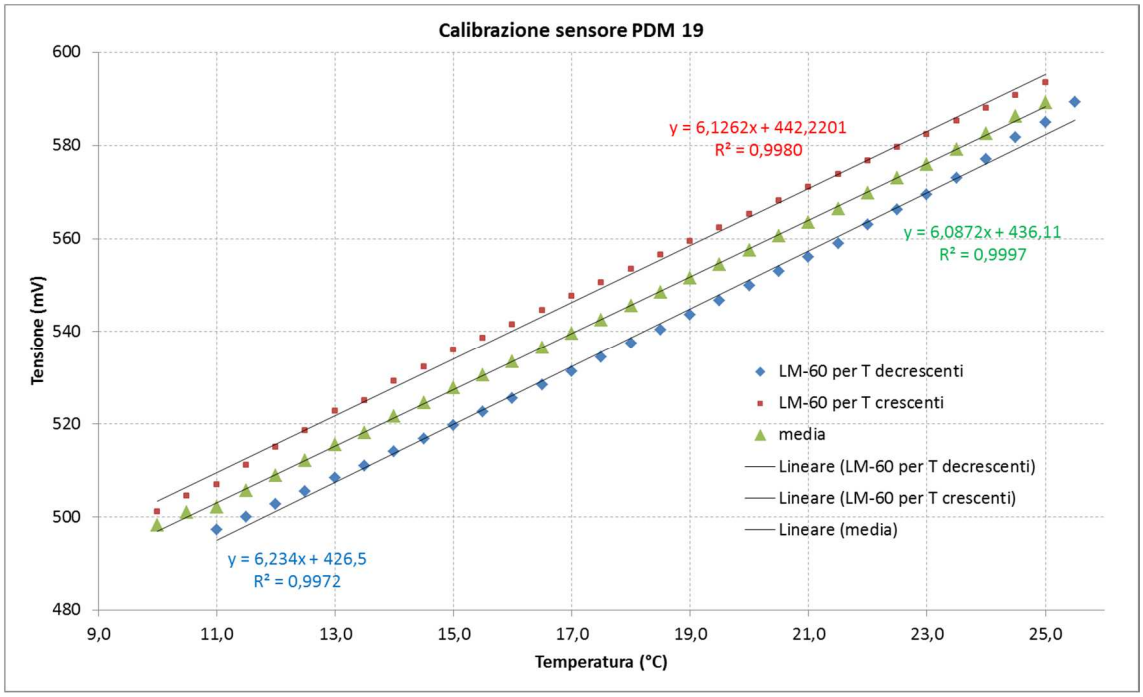

Fig. 30. Calibration curves for the LM-60 temperature sensor of the PDM 19.

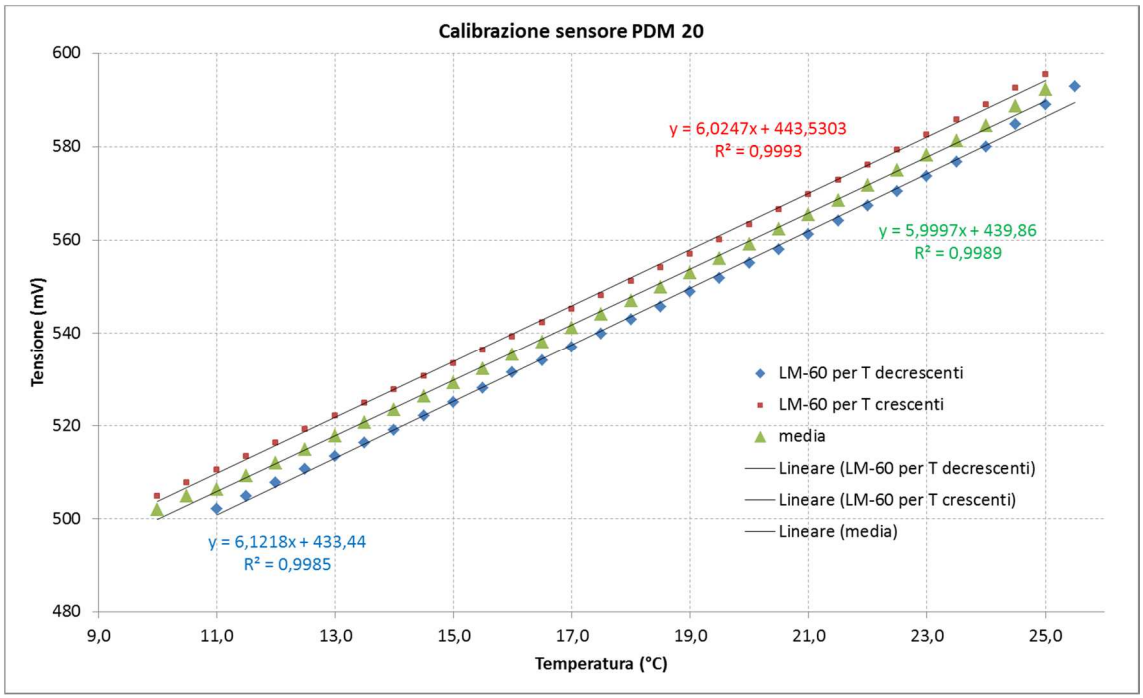

Fig. 31. Calibration curves for the LM-60 temperature sensor of the PDM 20.

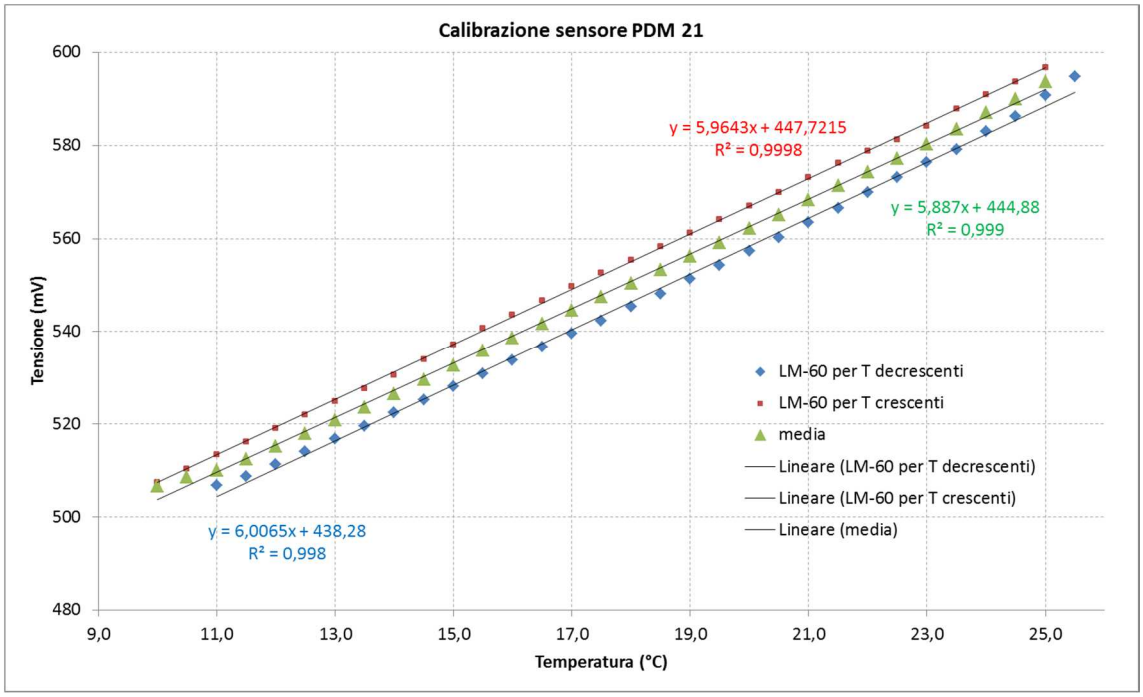

Fig. 32. Calibration curves for the LM-60 temperature sensor of the PDM 21.

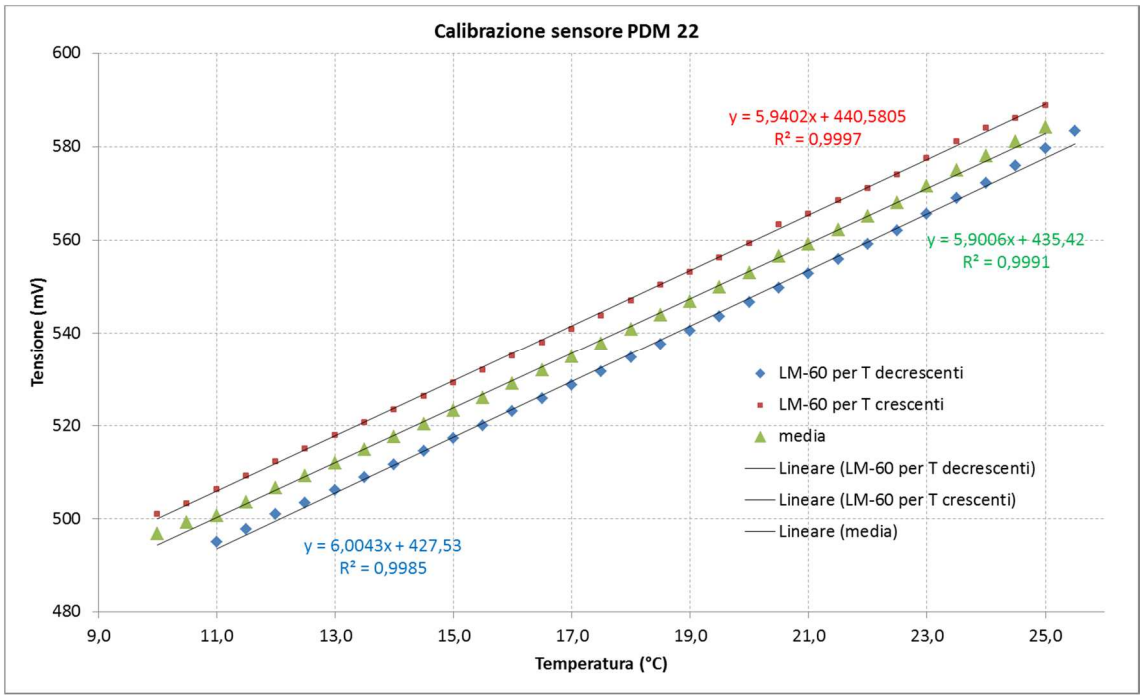

Fig. 33. Calibration curves for the LM-60 temperature sensor of the PDM 22.

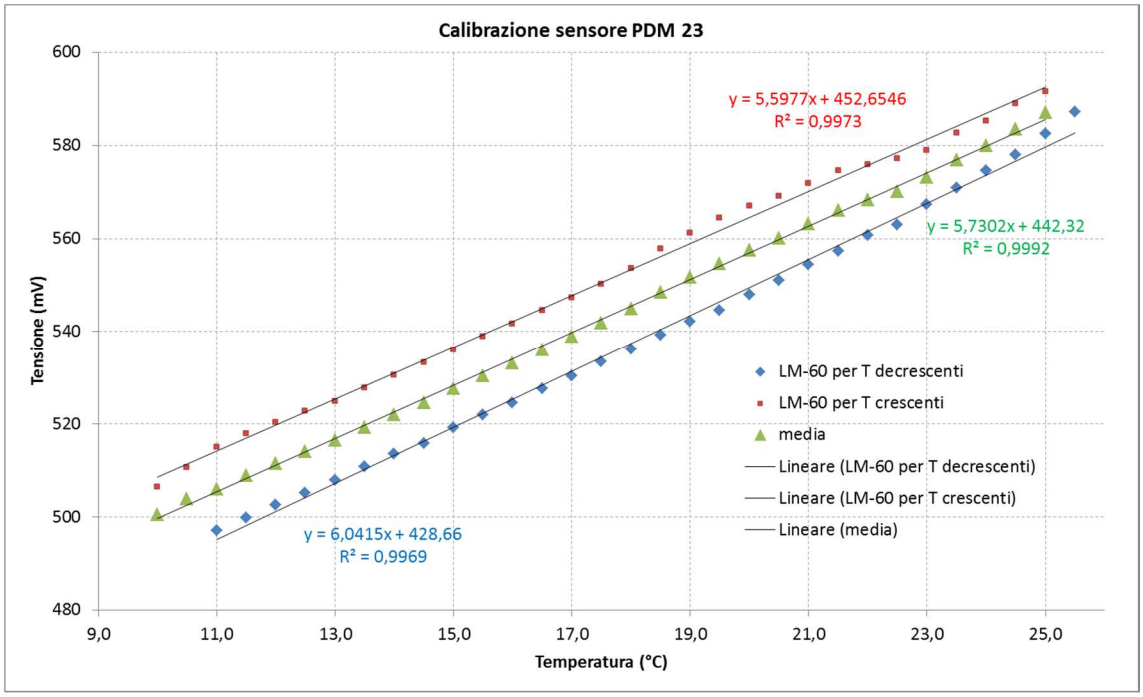

Fig. 34. Calibration curves for the LM-60 temperature sensor of the PDM 23.

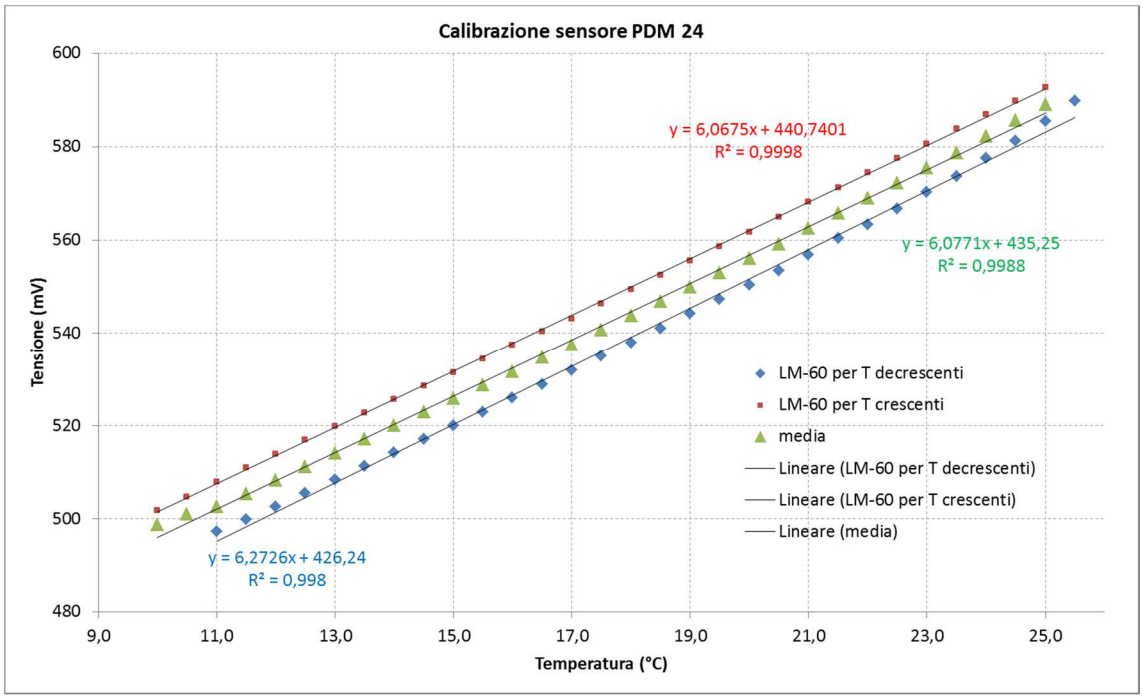

Fig. 35. Calibration curves for the LM-60 temperature sensor of the PDM 24.

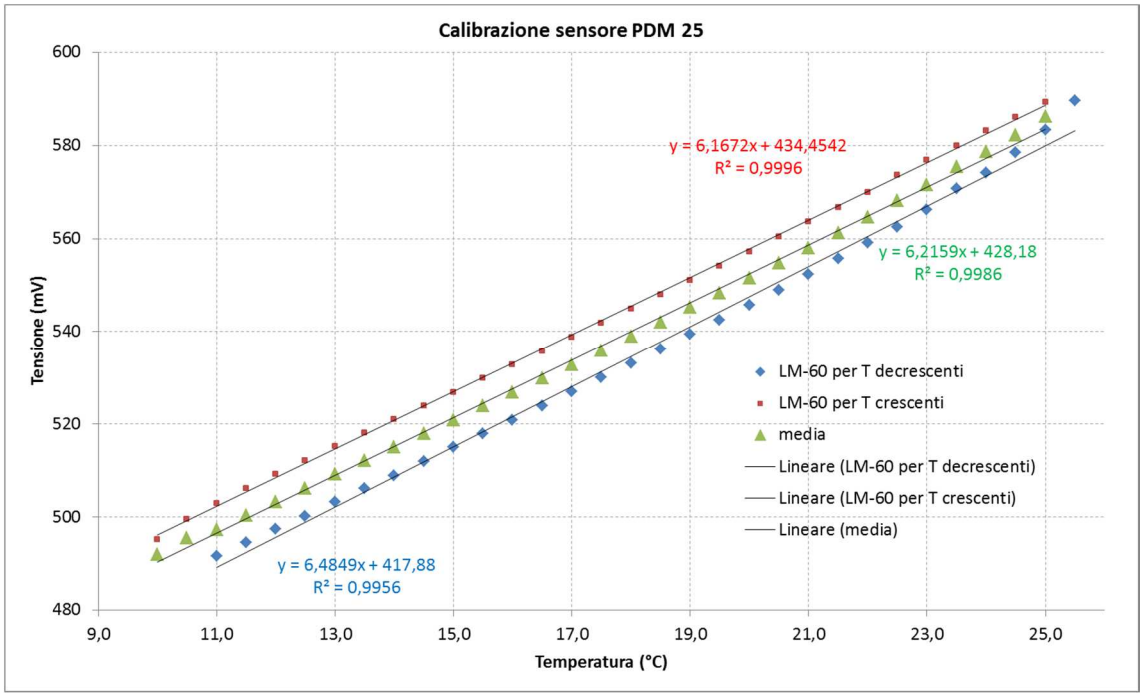

Fig. 36. Calibration curves for the LM-60 temperature sensor of the PDM 25.

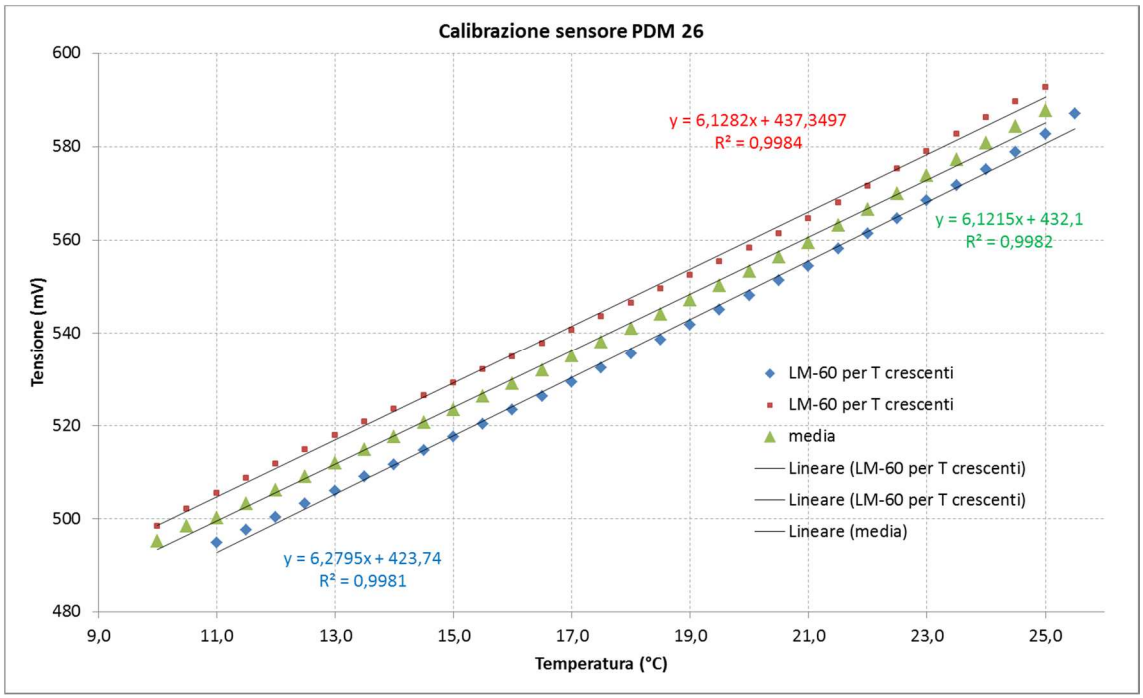

Fig. 37. Calibration curves for the LM-60 temperature sensor of the PDM 26.

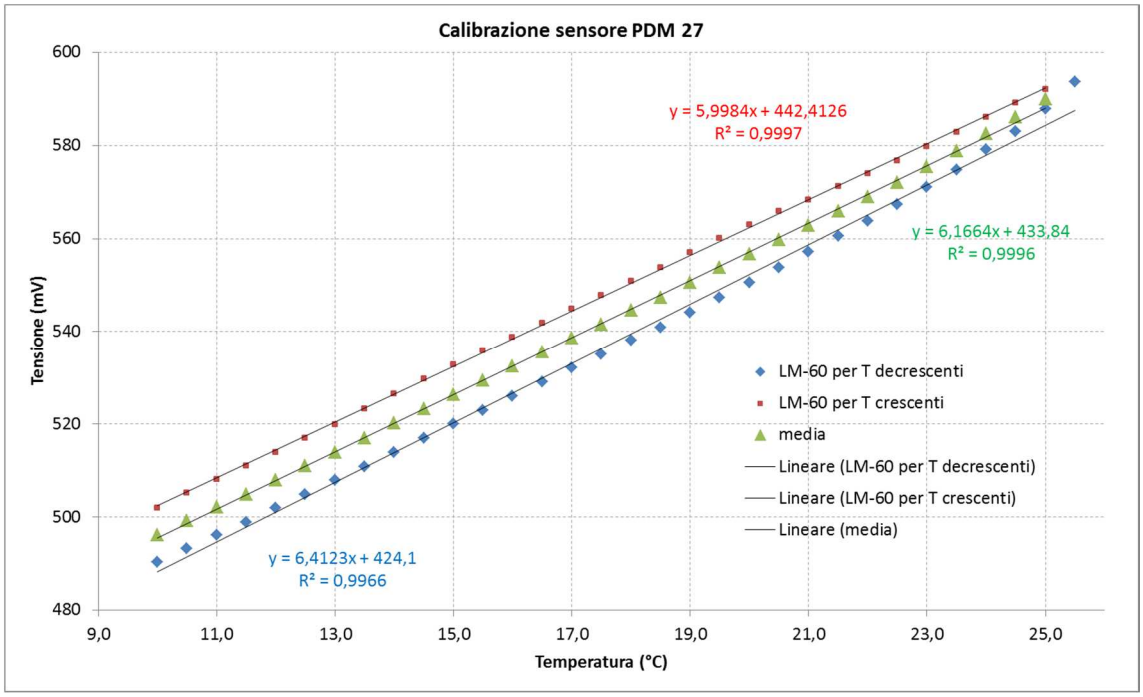

Fig. 38. Calibration curves for the LM-60 temperature sensor of the PDM 27.

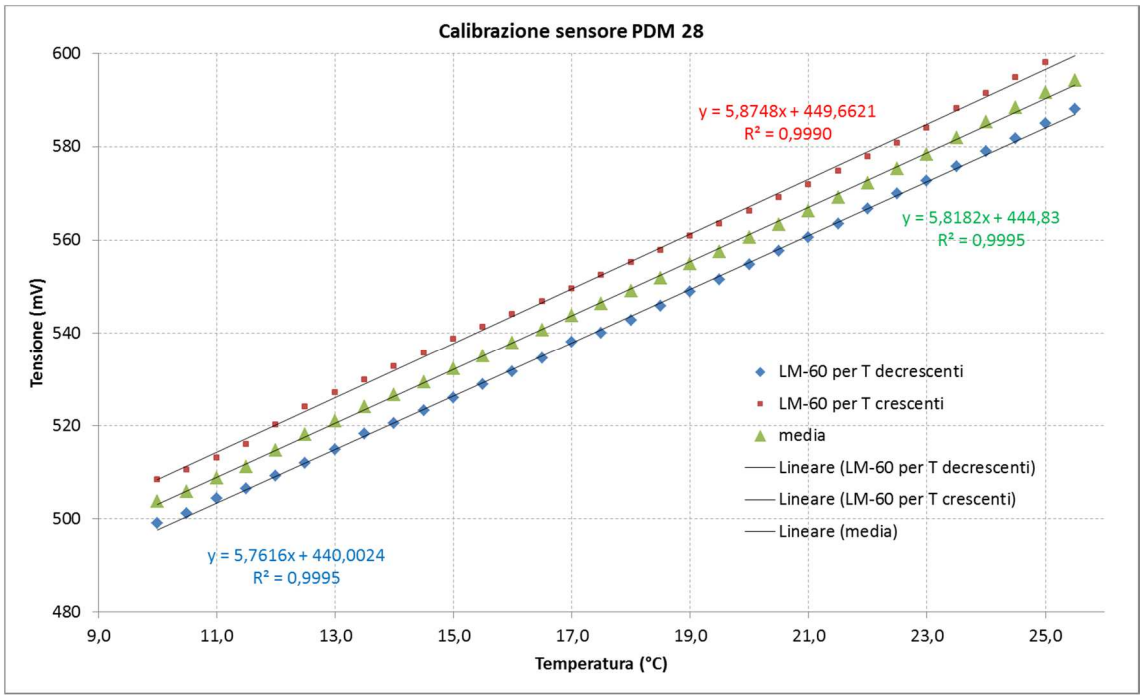

Fig. 39. Calibration curves for the LM-60 temperature sensor of the PDM 28.

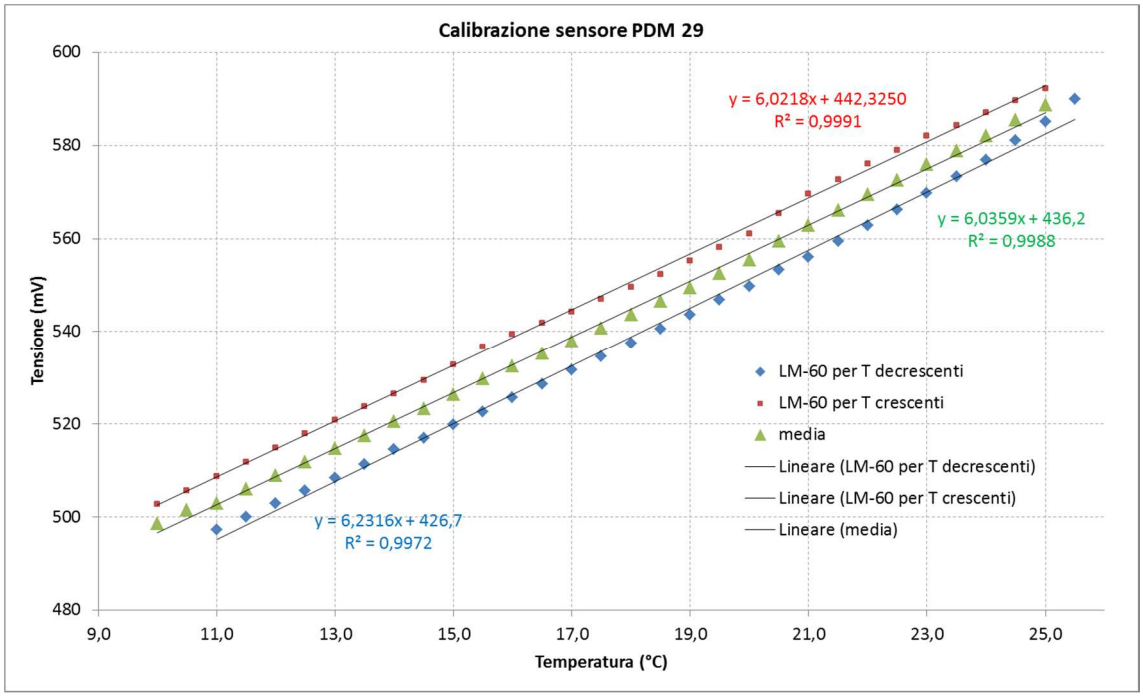

Fig. 40. Calibration curves for the LM-60 temperature sensor of the PDM 29.

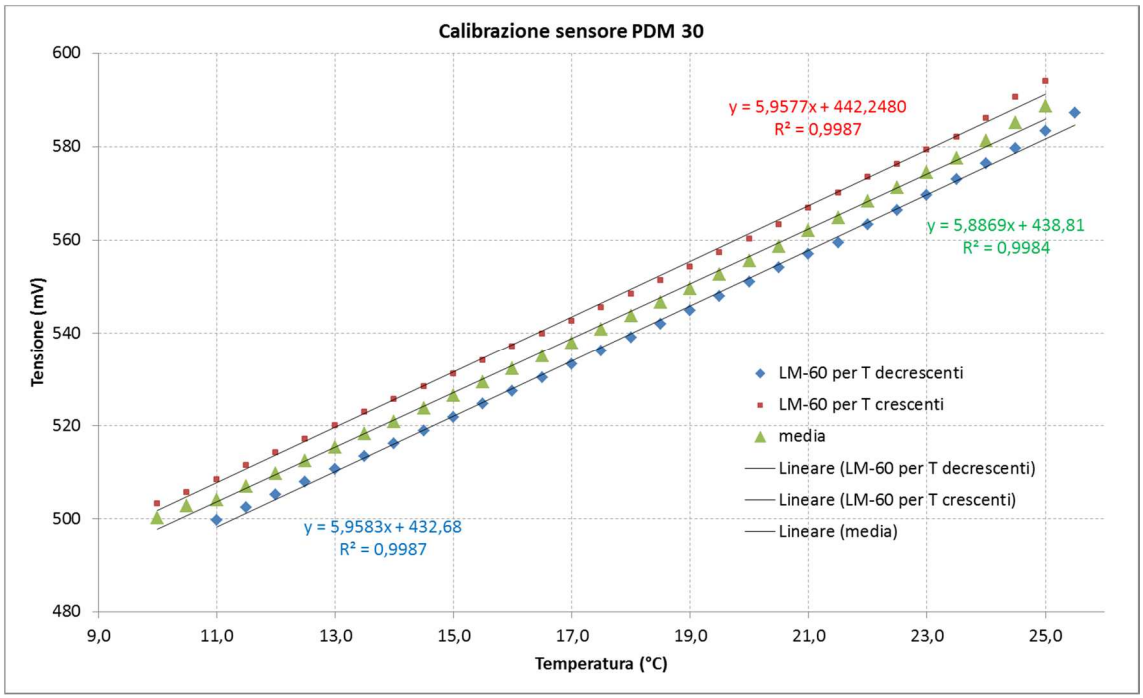

Fig. 41. Calibration curves for the LM-60 temperature sensor of the PDM 30.

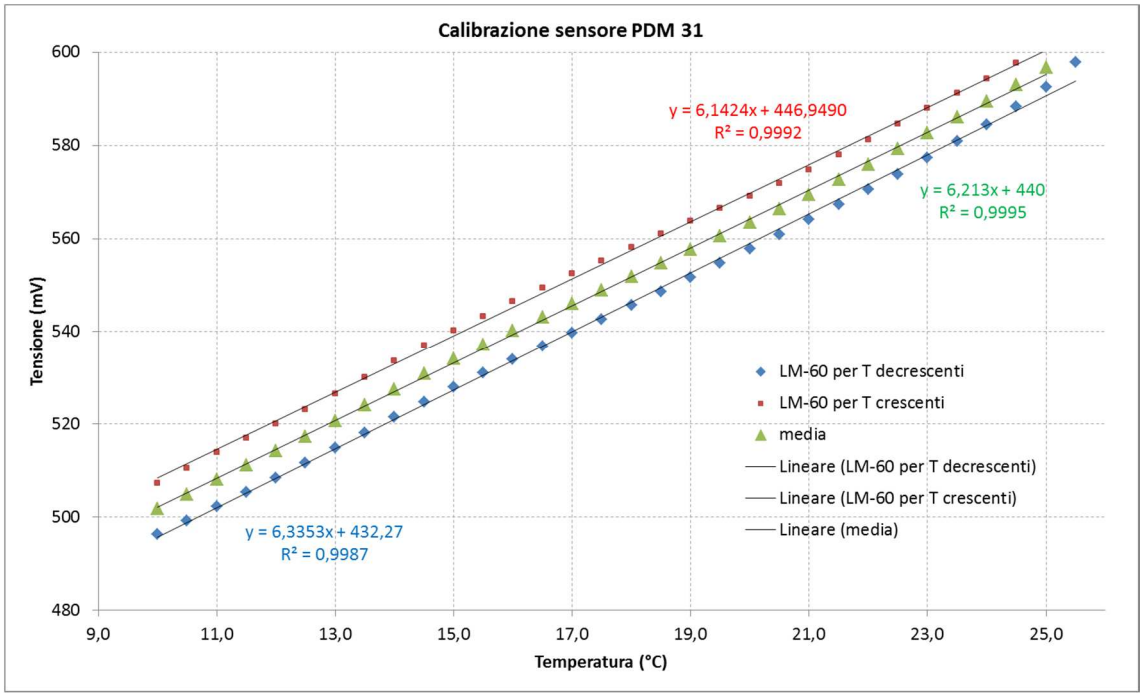

Fig. 42. Calibration curves for the LM-60 temperature sensor of the PDM 31.

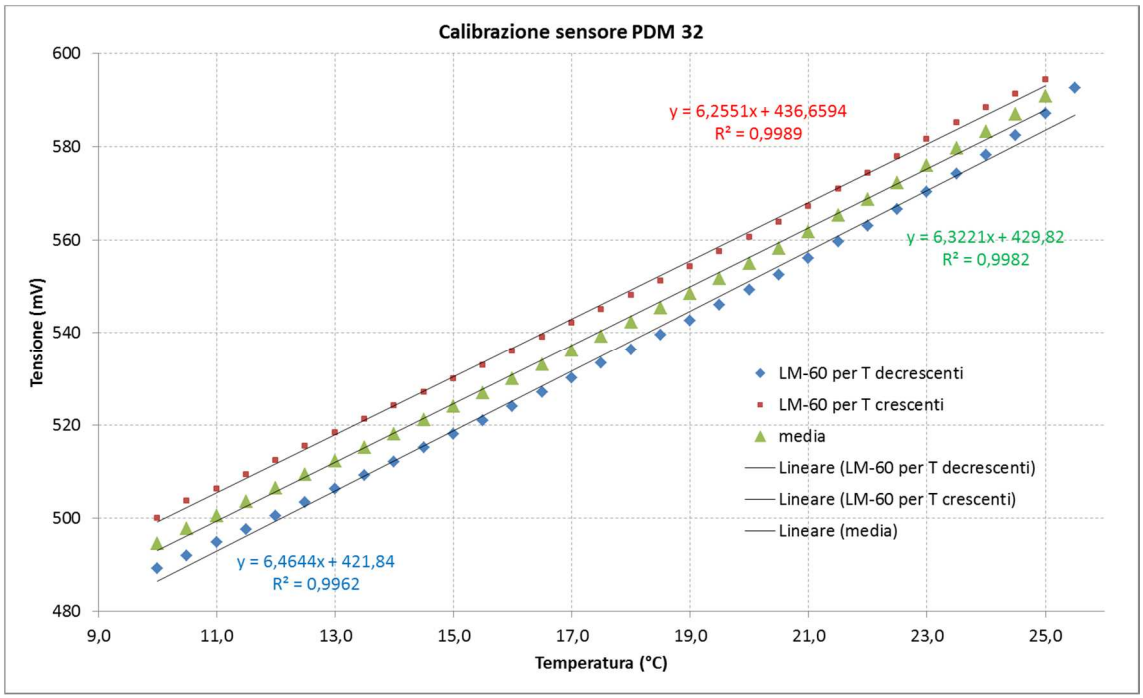

Fig. 43. Calibration curves for the LM-60 temperature sensor of the PDM 32.

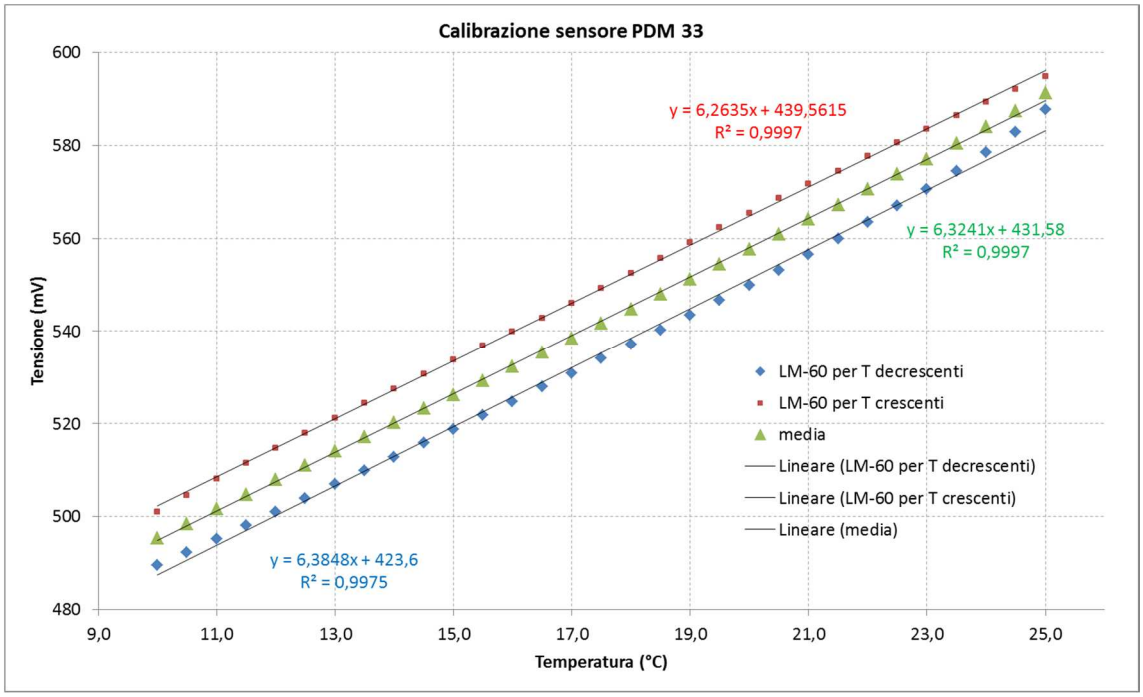

Fig. 44. Calibration curves for the LM-60 temperature sensor of the PDM 33.

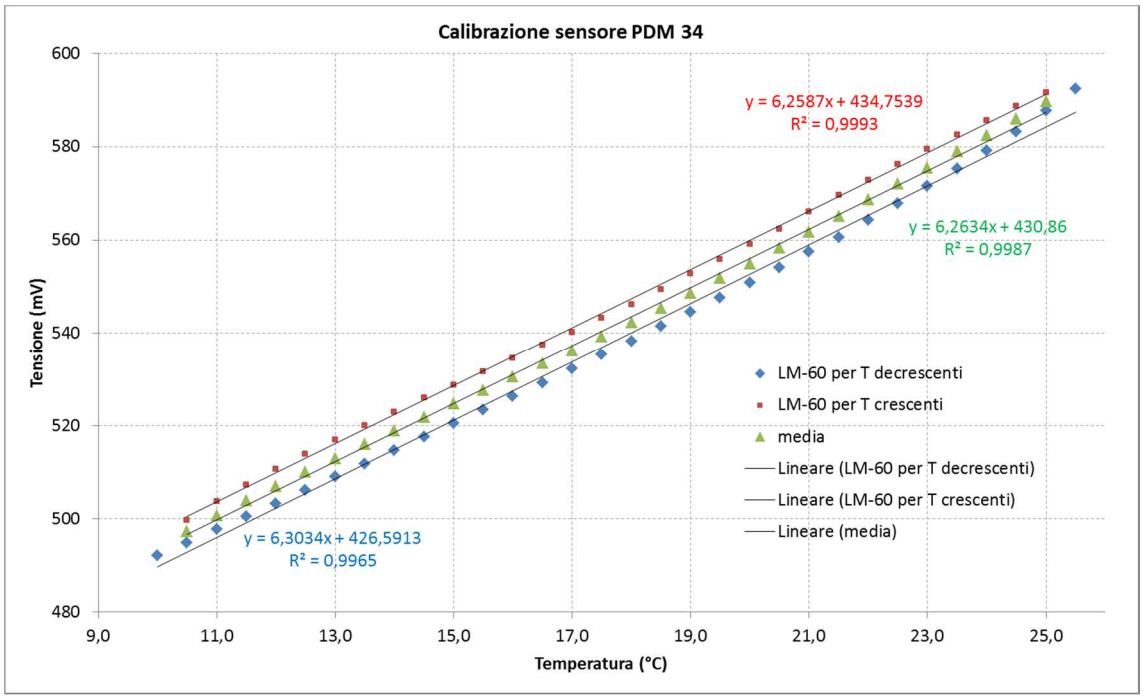

Fig. 45. Calibration curves for the LM-60 temperature sensor of the PDM 34.

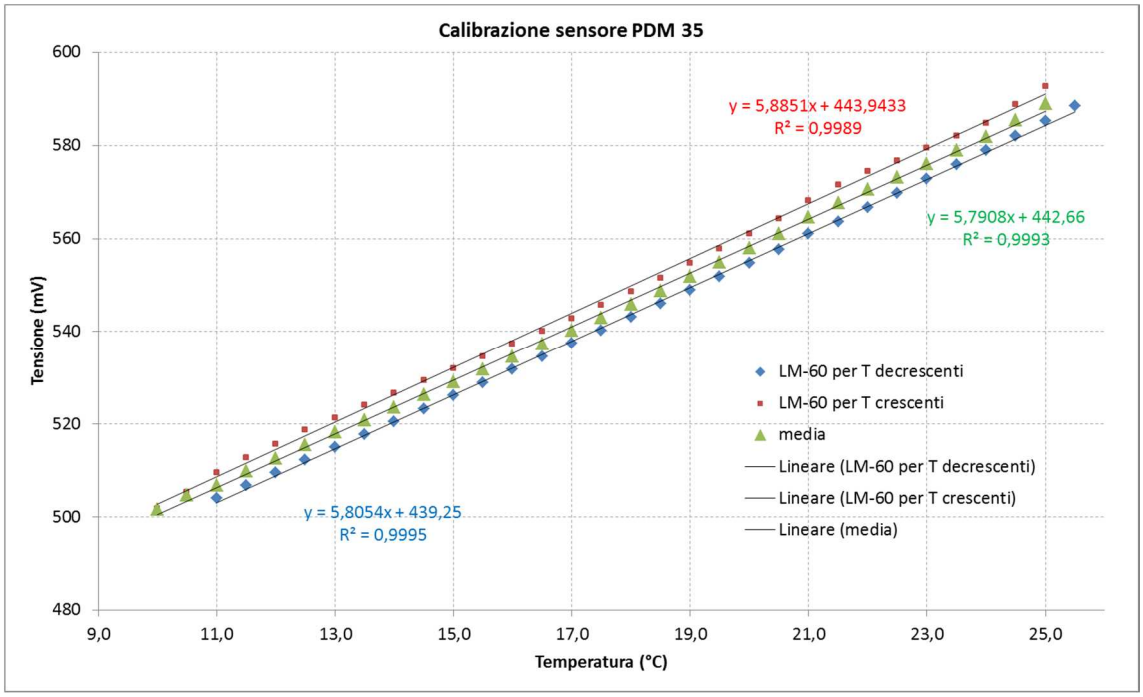

Fig. 46. Calibration curves for the LM-60 temperature sensor of the PDM 35.

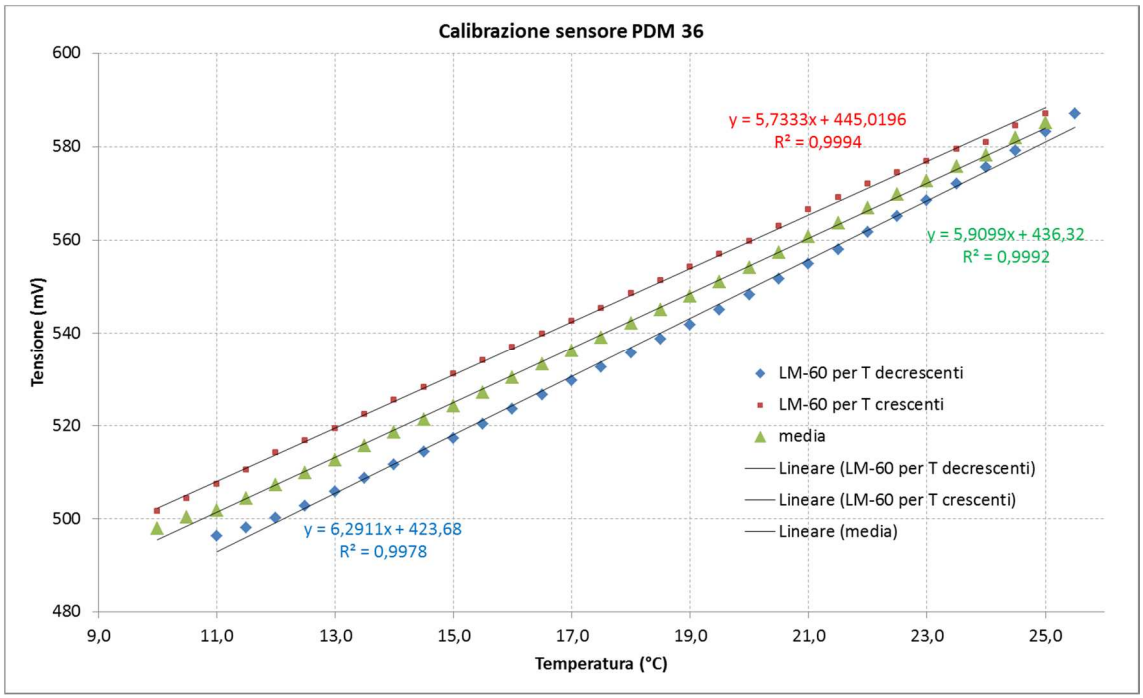

Fig. 47. Calibration curves for the LM-60 temperature sensor of the PDM 36.

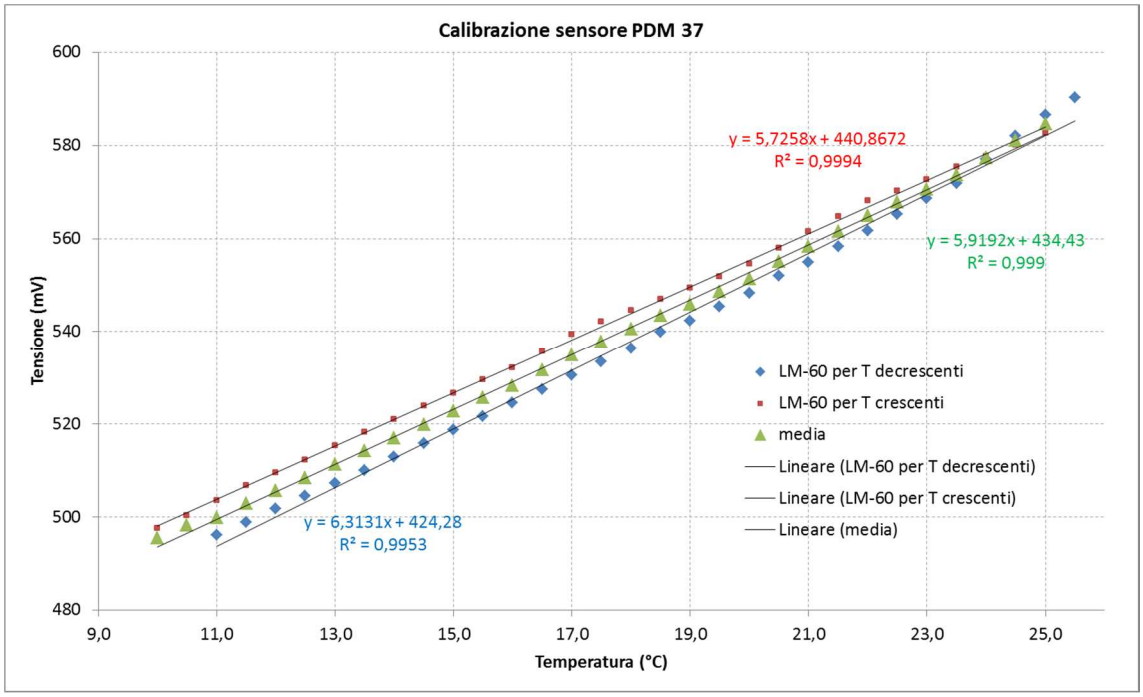

Fig. 48. Calibration curves for the LM-60 temperature sensor of the PDM 37.

In each of the above figures, the blue data represent the calibration points obtained for decreasing values of *T*, while the red data stand for those obtained for increasing *T*. Average data are also shown for each temperature.

Linear fits are reported for each set of measurements along with the relevant equations and errors.

For a specific temperature, the average difference between the highest and lowest data points in the above plots divided by the average slope of the linear fits is found to be approximately ±1.5°, representing the average accuracy of the LM-60 temperature sensor, which turns out to be compatible with the relevant value reported in the reference manufacturer datasheet [R1].

4. CONCLUDING REMARKS

Concerning the rising phase of measurements, for each fixed temperature in the most probable range of interest (13-17°C), the relevant voltage values in mV are plotted in the form of histograms for the 25 central PDMs in the focal plane reference scheme in Fig. 11, and the resulting plot is reported in Fig. *49*, showing the expected rising trend of the average acquired voltage with increasing temperature.

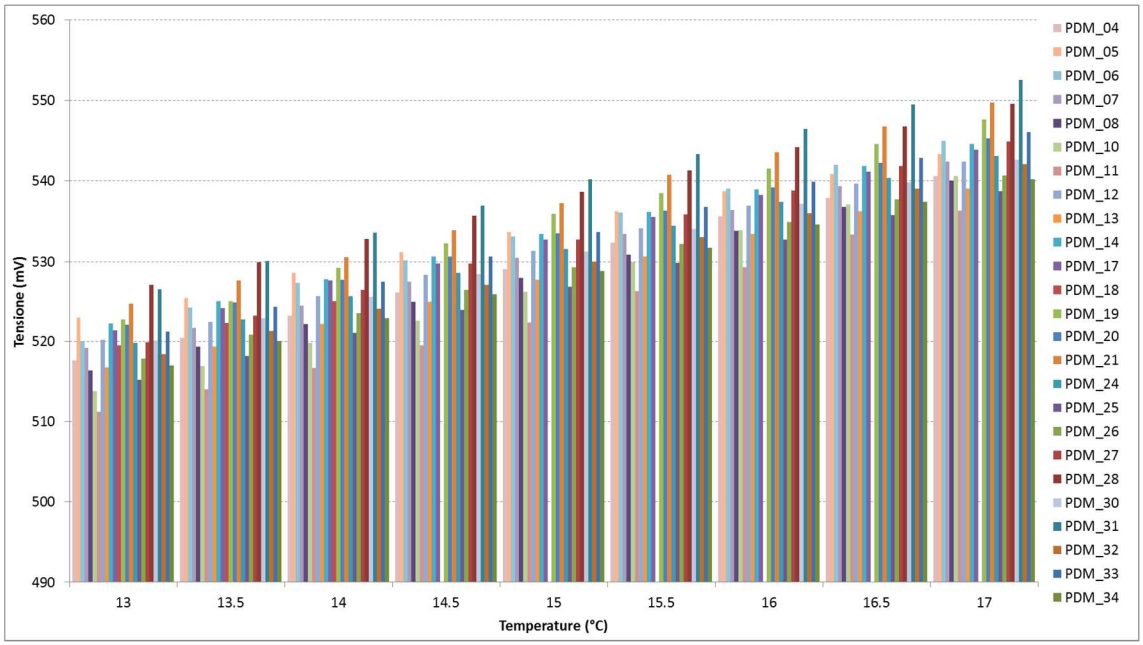

Fig. 49. Histograms of the acquired voltage values for each fixed temperature in the range of 13-17°C during the rising phase for the 25 central PDMs of the camera focal plane.

In the temperature range of 12-18°C, the calibration data points for all 37 PDMs of the camera focal plane are reported in the plot of Fig. 50, while the global linear fit along with its equation and errors are depicted in Fig. 51.

Due to the relatively large spread of the data points, for a fixed temperature, around the global linear fit (R^2=0.9026…), the slopes and *y*-axis intercepts of the 37 linear fits of the calibration data points in the 10-25°C range are provided in Table I, along with their average values and standard deviations.

As a final remark, calibration of the central sensor at the bottom of the SiPM board allows calibration of the other 8 sensors in the bottom side of the board to be easily accomplished with respect to the calibrated one.

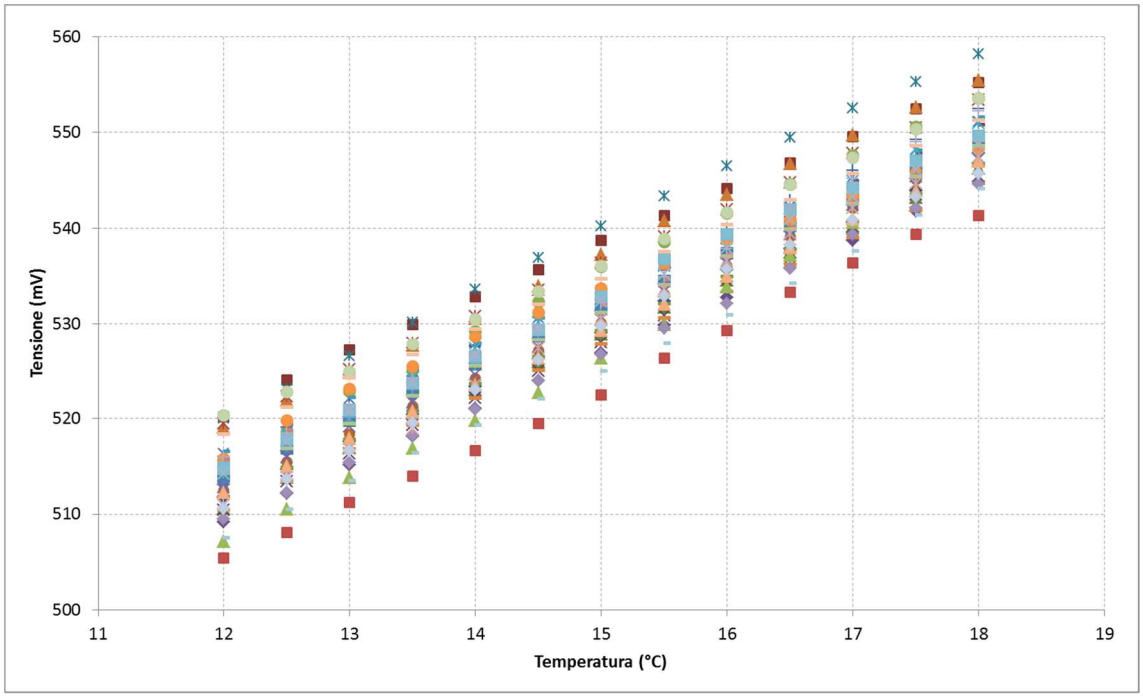

Fig. 50. Calibration data points in the range of 12-18°C for all 37 PDMs of the focal plane.

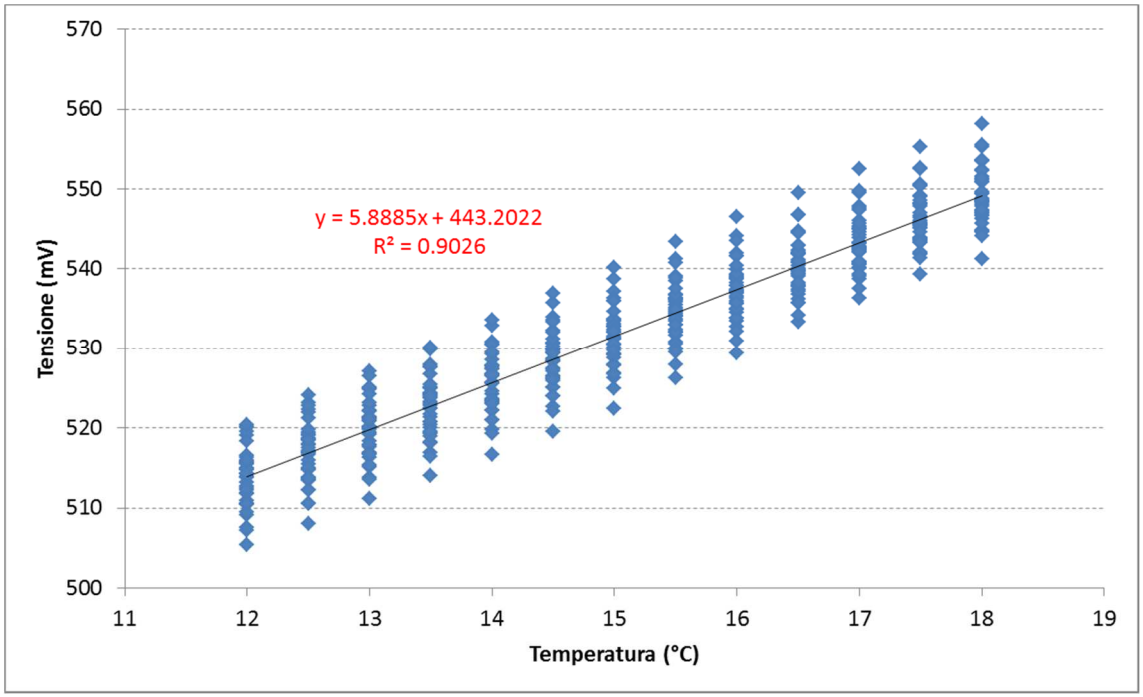

Fig. 51. Linear fit of the calibration data points in the range of 12-18°C for all 37 PDMs of the focal plane.

Table I. Slopes and *y*-axis intercepts of the 37 linear fits of the calibration data points.

	m (mV/°C)	q (mV)
PDM_01	5.9422	436.2092
PDM_02	5.7774	448.3038
PDM_03	5.7761	441.5572
PDM_04	5.9779	439.8559
PDM_05	5.6047	448.2146
PDM_06	6.1999	440.0811
PDM_07	6.0111	440.6008
PDM_08	6.4381	432.2498
PDM_09	5.7793	446.4512
PDM_10	6.3085	432.0625
PDM_11	5.8627	435.2466
PDM_12	5.8181	443.2881
PDM_13	5.9487	438.4023
PDM_14	5.9968	444.0432
PDM_15	5.9258	442.2859
PDM_16	5.9541	439.8885
PDM_17	5.6774	447.0672
PDM_18	5.9386	447.5459
PDM_19	6.1262	442.2201
PDM_20	6.0247	443.5303
PDM_21	5.9643	447.7215
PDM_22	5.9402	440.5805
PDM_23	5.5977	452.6546
PDM_24	6.0675	440.7401
PDM_25	6.1672	434.4542
PDM_26	6.1282	437.3497
PDM_27	5.9984	442.4126
PDM_28	5.8748	449.6621
PDM_29	6.0218	442.325
PDM_30	5.9577	442.248
PDM_31	6.1424	446.949
PDM_32	6.2551	436.6594
PDM_33	6.2635	439.5615
PDM_34	6.2587	434.7539
PDM_35	5.8851	443.9433
PDM_36	5.7333	445.0196
PDM_37	5.7258	440.8672
μ	5.9748649	441.81098
σ	0.1981636	4.9314731
σ/μ%	3.32%	1.12%

5. CONTACTS

The team working on the electronic design of the ASTRI camera is composed by people from INAF's Catania Astrophysical Observatory and Palermo IFC. It is also referred to as the Electronics Camera Team.

Giovanni Bonanno	gbo@oact.inaf.it	OACT Catania
Davide Marano	davide.marano@oact.inaf.it	OACT Catania
Giuseppe Romeo	giuseppe.romeo@oact.inaf.it	OACT Catania
Salvatore Garozzo	salvatore.garozzo@oact.inaf.it	OACT Catania
Alessandro Grillo	agrillo@oact.inaf.it	OACT Catania
Sergio Billotta	sergio.billotta@oact.inaf.it	OACT Catania
Osvaldo Catalano	osvaldo.catalano@iasf-palermo.inaf.it	IFC Palermo
Giovanni La Rosa	larosa@ifc.inaf.it	IFC Palermo
Giuseppe Sottile	sottile@ifc.inaf.it	IFC Palermo
Salvatore Giarrusso	jerry@ifc.inaf.it	IFC Palermo
Domenico Impiombato	domenico.impiombato@ifc.inaf.it	IFC Palermo